Editors' choice

New remains and paleoecology of uruguaytheriine astrapotheres (Mammalia) from the Middle Miocene of Bolivia

JULIA VAN ORMAN, OSCAR E. WILSON, ANGELINE CATENA, SMRUTHI MAGANTI, FEDERICO ANAYA, and DARIN A. CROFT

Van Orman, J., Wilson, O.E., Catena, A., Maganti, S., Anaya, F., and Croft, D.A. 2025. New remains and paleoecology of uruguaytheriine astrapotheres (Mammalia) from the Middle Miocene of Bolivia. *Acta Palaeontologica Polonica* 70 (3): 581–605.

Astrapotheres (Astrapotheria) are an order of South American native ungulates (SANUs), and the geologically youngest astrapotheres belong to the subfamily Uruguaytheriinae (Astrapotheriidae). In this study, we: (i) analyze uruguaytheriine remains from the late Middle Miocene Quebrada Honda Basin (QHB) of southern Bolivia; and (ii) discuss paleoecology of Bolivian astrapotheres based on new dental mesowear angle data and enamel stable carbon isotope ($\delta^{13}C$) data from these and other specimens. New material consists of a partial left maxilla preserving DP2–3 and an associated deciduous lower incisor. Two newly described specimens include a mostly complete m3 and a partial palate preserving left and right DP2–4. The QHB deciduous premolars are the first described for a uruguaytheriine and among the few described for astrapotheres. We conclude that the QHB specimens represent a new but unnamed species that likely does not pertain to any presently recognized genus. It differs from other uruguaytheriines in its intermediate size, relatively high-crowned teeth, presence of a lingually open M3 central valley, and absence of m3 hypoflexid, among other features. Astrapothere mesowear angle data from the QHB and slightly older Bolivian sites (Cerdas and Nazareno) suggest that Middle Miocene astrapotheres were browsers, perhaps resembling the extant black rhino (*Diceros bicornis*). New and updated enamel stable carbon isotope data suggest that QHB astrapotheres and toxodontid notoungulates fed on isotopically similar vegetation slightly more enriched (~1‰) than vegetation consumed by proterotheriid litopterns (*Olisanophus* spp.) and the notoungulate *Hemihegetotherium trilobus*. These data support paleopedology- and paleoichnology-based habitat reconstructions for the QHB that suggest it was more densely vegetated than Cerdas. Relatively enriched $\delta^{13}C$ samples (> -7.0‰) from Cerdas and Quehua (Late Miocene) suggest that some Bolivian notoungulates were grazing on C4 vegetation, which casts doubt on the proposal that the southern Central Andean Plateau experienced significant uplift prior to ~9 Ma.

Key words: Mammalia, Astrapotheria, carbon isotopes, mesowear, paleoelevation, Quebrada Honda Basin, Neogene, Neotropics, South America.

Julia Van Orman [jvanorma@macalester.edu; ORCID: https://orcid.org/0009-0007-6828-7254], Department of Biology, Macalester College, 1600 Grand Ave., Saint Paul, Minnesota, 55105, USA.

Oscar E. Wilson [oscar.wilson@helsinki.fi; ORCID: https://orcid.org/0000-0002-4046-3128], Department of Geosciences and Geography, University of Helsinki, P.O. Box 64 (Gustaf Hällströmin katu 2), 00014 Helsinki, Finland.

Angeline Catena [angeline.catena@case.edu; ORCID: https://orcid.org/0000-0003-0699-5726], Department of Physical Science, Diablo Valley Community College, Pleasant Hill, CA 94523, USA.

Smruthi Maganti [ssm103@case.edu; ORCID: https://orcid.org/0009-0007-9515-7295], Cleveland Clinic, 9500 Euclid Avenue, Cleveland, Ohio 44195, USA.

Federico Anaya [fedanaya@hotmail.com; ORCID: https://orcid.org/0009-0006-2821-9938], Facultad de Ingeniería Geológica, Universidad Autónoma "Tomás Frías", Av. del Maestro s/n, Potosí, Bolivia.

Darin A. Croft [dcroft@case.edu; ORCID: https://orcid.org/0000-0002-6514-2187], Department of Anatomy, School of Medicine, Case Western Reserve University, 10900 Euclid Ave., Cleveland, Ohio, 44106-4930, USA.

Received 24 December 2024, accepted 17 June 2025, published online 18 September 2025.

Introduction

Astrapotheria is an extinct order of South American native ungulates (SANUs) that inhabited the continent for much of the Paleogene and nearly half of the Neogene. The order has traditionally been divided into two families, Trigonostylopidae and Astrapotheriidae; however, the former seems to be a paraphyletic group of early-diverging astrapotheres (Soria 1984; Cifelli 1993; Kramarz and Bond 2011; Kramarz et al. 2019). The family Astrapotheriidae includes a series of early-diverging stem taxa (e.g., *Albertogaudrya*, *Astraponotus*, *Maddenia*, *Parastrapotherium*) and two well-defined sister-clades, Astrapotheriinae and Uruguaytheriinae (Cifelli 1993; Johnson and Madden 1997; Kramarz and Bond 2009, 2011; Vallejo-Pareja et al. 2015; Carrillo et al. 2018).

The subfamily Astrapotheriinae includes the Early Miocene to early Middle Miocene genera *Astrapothericulus* and *Astrapotherium*. Fossil occurrences are restricted to southern South America, mainly Patagonia (e.g., Scott 1928, 1937; Kraglievich 1930; Cabrera 1940; Marshall et al. 1990; Kramarz 2009; Kramarz and Bond 2010). Remains referred to cf. *Astrapotherium* from the Aisol Formation in Mendoza province, Argentina (~35°S; Soria 1983; Forasiepi et al. 2011) currently represent the northernmost record of astrapotheriines.

The subfamily Uruguaytheriinae includes three Early to Middle Miocene genera known exclusively from tropical latitudes (*Granastrapotherium*, *Hilarcotherium*, and *Xenastrapotherium*) plus *Uruguaytherium*, a late Oligocene genus presumably from the Fray Bentos Formation of Uruguay and northeast Argentina (Johnson and Madden 1997; Kramarz and Bond 2011; Vallejo-Pareja et al. 2015; Carrillo et al. 2018; see also below).

The best-characterized representative of the order is *Astrapotherium magnum* from the late Early Miocene Santa Cruz Formation of Argentina, which is known from many specimens, including a nearly complete skeleton (Riggs 1935; Scott 1937; Cassini et al. 2012). Other astrapotheres are known almost exclusively from craniodental material, though some specimens are well-preserved and relatively complete (e.g., Johnson and Madden 1997; Kramarz et al. 2011, 2019). Astrapotheres are characterized by a diastema separating their well-developed, tusk-like canines from their premolars, and they lack upper incisors (Johnson 1984). Sexual dimorphism in tusk morphology has been proposed for one species (Johnson and Madden 1997). Retracted nasal bones in many astrapotheres suggest the presence of a tapir-like proboscis in life (Scott 1928; Wall 1980). Late Oligocene and Neogene species were generally quite large (> 1000 kg; Kramarz and Bond 2011; Cassini et al. 2012; Croft 2016; Carrillo et al. 2018).

Remains of astrapotheres are often found in riverine sedimentary layers, which has led to the hypothesis that they preferred moist, lowland environments and may have been semi-aquatic (Riggs 1935; Marshall et al. 1990; Weston et al. 2004). Although astrapotheres have no obvious postcranial adaptations for a semi-aquatic lifestyle, the size and proportions of the limbs of *Astrapotherium* have been likened to those of the Indian rhinoceros (*Rhinoceros unicornis*; Cassini et al. 2012), which inhabits alluvial plain grasslands and is an excellent swimmer (Laurie et al. 1983; Nowak 1991). Houssaye et al. (2016) concluded that the long bone microstructure of late Oligocene *Parastrapotherium* suggests semi-aquatic habits.

Astrapotheriids were widespread in South America during the Oligocene and Early Miocene but became restricted to lower latitudes during the Middle Miocene (see Croft et al. 2016 and references therein). The most complete astrapothere material from southern South America during this interval is the recently described *Astrapotherium guillei* from the Collón Cura Formation of Río Negro province in northwest Patagonia (Kramarz et al. 2019). These deposits lack secure age control, but an $^{40}Ar/^{39}Ar$ date of 15.7 Ma has been reported by Madden et al. (1997) for the Pilcaniyeu Ignimbrite. This layer underlies the Las Bayas member, which has yielded most Collón Cura Formation fossils in the area, including *A. guillei* (Bondesio et al. 1980; Kramarz et al. 2019). The only other astrapothere remains from southern South America that may be of similar (i.e., Middle Miocene) age are fragmentary specimens referred to *Astrapotherium hesperinum* from the Río Frías and Collón Cura formations (Kraglievich 1930; Cabrera 1940; Kramarz et al. 2019).

In stark contrast to southern South America, Middle Miocene deposits in equatorial South America are replete with astrapotheriid fossils (e.g., Johnson and Madden 1997; Goillot et al. 2011; Vallejo-Pareja et al. 2015; Carrillo et al. 2018; Croft et al. 2020b). These remains all correspond to uruguaytheriines, as do all Oligocene and Miocene remains from low-latitude South America; no astrapotheriines or earlier-diverging astrapotheres have been discovered north of ~17°S (the latitude of the late Oligocene site of Salla, Bolivia; MacFadden et al. 1985). A lower incisor and canine from the late Oligocene site of Tremembé, Brazil (~23°S) was recently referred to the subfamily Astrapotheriinae by Carmo et al. (2024), but since no justification was provided for this identification, its accuracy cannot be evaluated. Definitive uruguaytheriines have only been documented from tropical latitudes (i.e., north of 23.5°S), with the obvious exception of the geologically oldest member of the clade, *Uruguaytherium beaulieui*. The holotype of *U. beaulieui* was collected in the department of Río Negro in western Uruguay (~33°S; Kraglievich 1928). Although its exact provenance is unknown, it likely derives from the Fray Bentos Formation (Mones and Ubilla 1978), which has produced remains of several other types of mammals (e.g., Reguero et al. 2003; Perea et al. 2014) and also crops out in the provinces of Corrientes and Entre Ríos in northeast Argentina (Bond et al. 1998). The Fray Bentos Formation lacks radiometric age control but is generally regarded as late Oligocene in age based on its mammal fauna (Deseadan SALMA; Zurita et al. 2016; Cerdeño et al. 2020). No specimen of *U. beaulieui* other than the holotype has been reported from Uruguay, but isolated teeth have been question-

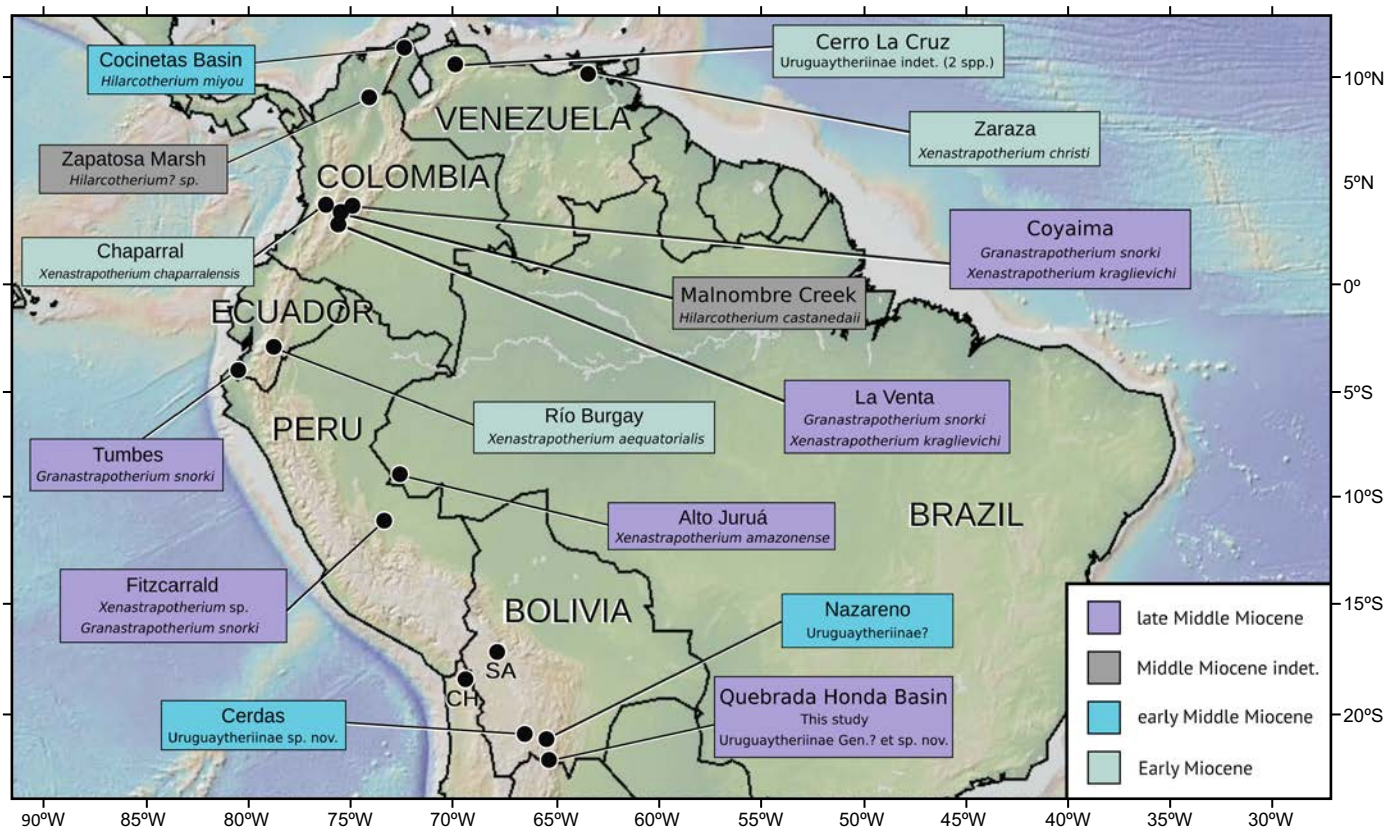

Fig. 1. Map of northern South America (above 25°S), showing sites that have produced Miocene astrapothere remains. Colors indicate age: Green, Early Miocene; blue, early Middle Miocene; purple, late Middle Miocene; grey, unknown age. Localities: Alto Juruá (Paula Couto 1976, 1982; Ranzi 1981; Negri et al. 2010); Cerdas (Croft et al. 2016); Cerro La Cruz (Weston et al. 2004, with taxonomy modified following Kramarz and Bond 2009); Chaparral (Johnson and Madden 1997); Fitzcarrald (Antoine et al. 2007; Goillot et al. 2011); Cocinetas Basin (Carrillo et al. 2018); Coyaima (Johnson and Madden 1997; OEW personal observation); La Venta (Cabrera 1929; Johnson 1984); Malnombre Creek (Vallejo-Pareja et al. 2015); Nazareno (Croft and Anaya 2020; present study); Quebrada Honda Basin (Hoffstetter 1977; Frailey 1987); Río Burgay (Johnson and Madden 1997); Tumbes (Croft et al. 2020b); Zapatosa Marsh (Pardo-Jaramillo 2018); Zaraza (Kraglievich 1928; Stehlin 1928). The site of late Oligocene Salla (SA) and the late Early Miocene site of Chucal (CH), which are mentioned in the text, are also shown.

ably referred to the genus from exposures of the Fray Bentos Formation in Argentina (Bond et al. 2001; Roig et al. 2024).

The most significant astrapotheriid region in northern South America is La Venta, Colombia and surrounding sites (Fig. 1), where extensive outcrops of the late Middle Miocene-aged La Victoria and Villavieja formations are exposed (Kay et al. 1997; Carrillo et al. 2023). Three astrapotheriid species have been identified from this area (*Xenastrapotherium kraglievichi*, *Granastrapotherium snorki*, and *Hilarcotherium castanedaii*), a greater number than at most fossil sites. Astrapothere remains are generally abundant and well-preserved at La Venta and have provided important insights into the paleoecology of Middle Miocene astrapotheres (Johnson 1984; Johnson and Madden 1997; Vallejo-Pareja et al. 2015; Croft et al. 2020b).

Four species have been referred to the genus *Xenastrapotherium* in addition to *X. kraglievichi* from La Venta, making it the most diverse and widely distributed uruguaytheriine genus. The type species, *Xenastrapotherium christi*, is based on a mostly complete mandible collected nearly a century ago from Zaraza, Venezuela (Stehlin 1928). Other species include *Xenastrapotherium amazonense* from western Brazil, *Xenastrapotherium chaparralensis* from central Colombia, and *Xenastrapotherium aequatorialis* from Ecuador (Cabrera 1929; Stirton 1947; Paula Couto 1976; Johnson and Madden 1997; Goillot et al. 2011; Fig. 1). The genus *Granastrapotherium* is monospecific but was relatively widespread during the late Middle Miocene; specimens likely referable to *G. snorki* have been reported from northern and central Peru in addition to La Venta and Coyaima, another site in the Magdalena River Valley of Colombia that is slightly lower stratigraphically than La Venta (Johnson and Madden 1997; Tejada-Lara et al. 2015; Croft et al 2020b). *Hilarcotherium castanedaii* is known only from the type locality (Malnombre Creek), but a second species, *Hilarcotherium miyou*, was referred to the genus by Carrillo et al. (2018) from the slightly older (early Middle Miocene) Castilletes Formation of the Cocinetas Basin of northern Colombia (Carrillo et al. 2018).

The intermediate latitudes of South America (i.e., between ~15°S and ~30°S) represent the biogeographic transition zone between uruguaytheriine-dominated faunas in the north and those occupied by other astrapotheres in the south. Unfortunately, astrapothere remains from this

region are scarce, and the few that have been described are not sufficiently complete for precise identification. We are aware of only three astrapothere specimens that have been discovered at Salla in western Bolivia (Fig. 1), one of the most productive late Oligocene terrestrial mammal sites in South America (e.g., Patterson and Wood 1982; MacFadden et al. 1985; Marshall and Sempere 1991; Shockey and Anaya 2008; Billet et al. 2009; Croft 2016): a lower canine in the collections of the University of Florida (Bruce Shockey, personal communication 2024), an incisor in the collections of the Museo Nacional de Historia Natural in La Paz, Bolivia (Shockey 1997: 76), and a few undescribed canine and upper molar fragments in the Muséum national d'Histoire naturelle in Paris, France (OEW, personal observation). The sole Early Miocene site from this region of South America, Chucal in northern Chile (~18.75°S; Fig. 1), has yet to yield astrapothere remains (Flynn et al. 2002; Croft et al. 2004, 2007; Croft 2016). By contrast, three Middle Miocene sites in Bolivia have produced astrapothere fossils. Croft et al. (2016) referred teeth and tooth fragments from the early Middle Miocene site of Cerdas to a new (but unnamed) species of uruguaytheriine. Astrapothere remains from the likely contemporaneous site of Nazareno were reported by Croft and Anaya (2020: table 1). A posterior cranium from the late Middle Miocene site of Quebrada Honda (here referred to as the Quebrada Honda Basin or QHB) was questionably referred to *Xenastrapotherium* by Frailey (1987). The astrapothere remains from the QHB are noteworthy, along with those from La Venta, in being the geologically youngest astrapothere fossils with secure absolute age constraints (Johnson and Madden 1997; Croft 2007; Croft et al. 2020a). Thus, they are vital for understanding the dénouement of the order Astrapotheria.

In this contribution, we provide the first descriptions of astrapothere dental remains from the QHB, which provide new taxonomic information about this late Middle Miocene astrapothere. These remains include: a maxilla fragment bearing two deciduous premolars and an associated incisor collected by a joint CWRU and UATF team in 2016 (UATF-V-002013); previously undescribed tooth fragments that Hofstetter (1977) referred to "*Uruguaytherium*–*Xenastrapotherium*" (MNHN.F.BLV46); and a partial rostrum with deciduous premolars collected by one of us (FA) in 1994 (MNHN-BOL-V-003672). We compare these dental specimens to the edentulous posterior cranium described by Frailey (1987) and tooth fragments associated with that specimen (UF 26679) and conclude that all specimens pertain to a single, previously undocumented astrapothere species. These remains are insufficient for naming a new species but reinforce the distinctiveness of the QHB's mammal fauna relative to that of La Venta. We also discuss the paleobiology of Middle Miocene astrapotheres by integrating new dental mesowear data and new enamel stable carbon isotope ($\delta^{13}C$) data from specimens from the QHB and other Middle Miocene Bolivian sites.

Institutional abbreviations.—IGM, Museo Geológico José Royo y Gómez, Servicio Geológico Colombiano, Bogotá, Colombia; MNHN, Muséum national d'Histoire naturelle, Paris, France; MNHN-BOL-V, Vertebrate Paleontology Collections, Museo Nacional de Historia Natural, La Paz, Bolivia; UATF-V, Vertebrate Paleontology Collections, Universidad Autónoma Tomás Frías, Potosí, Bolivia; UF, University of Florida/Florida Museum of Natural History, Gainesville, Florida, USA.

Other abbreviations.—Ch., character; DP/dp, deciduous upper/lower premolar; M/m, upper/lower molar; MA, mesowear angle; MAAT, mean annual air temperature; P/p, upper/lower premolar; QHB, Quebrada Honda Basin; SANU, South American native ungulates.

Material and methods

UATF-V-002013 (the new specimen described below) was prepared in the Vertebrate Paleontology Lab at the Cleveland Museum of Natural History (Cleveland, Ohio). The maxilla was scanned at The University of Chicago's PaleoCT lab (Chicago, Illinois) using a GE dual tube micro X-ray computed tomography (CT) scanner at 120kV and 350uA. This generated 1 961 slices with a voxel size of 42.4 μm.

Astrapothere dental terminology follows Kramarz and Bond (2009) and the character and state descriptions of Kramarz et al. (2019). Mesiodistal and buccolingual diameters were measured as the maximum occlusal diameter. Specimens studied firsthand were measured to the nearest 0.1 mm using a Mitutoyo absolute digimatic calipers. Other specimens were measured on digital photos to the nearest 0.1 mm using ImageJ software (Schneider et al. 2012), or measurement values were taken from the cited literature. Specimens were photographed using a Pentax K10 digital camera with a Pentax-D FA 50 mm F2.8 macro lens and model AF160FC lens-mounted ring flash.

To investigate the dietary ecology of Middle Miocene Bolivian astrapotheres, we applied mesowear angle (MA) techniques, as described by Wilson et al. (2024) and Wilson and Saarinen (2024b) for toxodontid and leontiniid notoungulates. Astrapotheres have an ectolophodont molar morphology, analogous to that of rhinoceroses, so angles that have been applied in rhinoceroses should be applicable to this group as well. Since few Middle Miocene astrapothere remains are known from the QHB, we also include specimens from the early Middle Miocene site of Cerdas (MacFadden et al. 1995; Croft et al. 2009, 2016) and the Middle Miocene site of Nazareno (Oiso 1991; Croft et al. 2016; Croft and Anaya 2020).

To measure MAs, astrapothere specimens were scanned with the Polycam 3D scanning application (Polycam 2024) using the photogrammetry mode. Scans were saved as .obj files, and MAs were measured manually in Blender v3.1.0 (Blender Online Community 2022) using slightly differ-

ent methods for lower and upper molars. For lower molar fragments (UATF-V-001052 and UATF-V-001054 from Nazareno and UATF-V-001981 from Cerdas; the lower molars of MNHN.F.BOL.46 do not preserve wear facets), we used the lower molar facet angle of Hernesniemi et al. (2011), measuring the angle of the wear facet on the buccal side of the tooth relative to the external surface at the level of the hypoconid and protoconid. It was not possible to determine the mesiodistal position of the facet in UATF-V-001981 due to its fragmentary state, but we have nonetheless included it here, since we have found facet angles to be consistent along the length of the tooth in astrapotheres and other taxa we have analyzed. In extant rhinos, greater angles in the lower teeth indicate better-developed wear facets, which are typical of browsers (Hernesniemi et al. 2011). For upper teeth (UATF-V-002013, MNHN.F.BLV 46, and UF 26679 from the QHB; we were unable to measure this angle in MNHN-BOL-V-003672 or UF 563068), we measured the facet inclination (FI) at the level of the paracone and metacone (or only one of the two where both were not available) as the angle of the wear facet of the ectoloph relative to the rest of the occlusal surface of the tooth. This facet inclination was then converted to a mesowear angle (MA) following the equation MA = 180° – (2 × FI) (Xafis et al. 2020; Saarinen and Lister 2023; Wilson and Saarinen 2024b; Wilson et al. 2024). In extant mammals, lower MA values in upper teeth are consistent with a less abrasive diet, typically associated with browsing.

MacFadden et al. (1994) published enamel stable carbon isotope ($\delta^{13}C$, ‰, relative to the Vienna PeeDee Belemnite) values for four QHB herbivores, including one astrapothere (UF 26679, described by Frailey 1987), three toxodontid notoungulates, and a hegetotheriid notoungulate (*Hemihegetotherium trilobus*). We broaden this QHB sample with new enamel $\delta^{13}C$ data from proterotheriid litopterns (*Olisanophus* spp.; n = 4) and additional specimens of toxodontids (n = 7) and *H. trilobus* (n = 5). Analyses were performed at the University of Utah Stable Isotope Ratio Facility for Environmental Research. Enamel samples from these notoungulates and litopterns were serially sampled following the methods of MacFadden and Higgins (2004) and Cerling et al. (2013, 2015). Between 0.1 and 0.2 mg of powdered enamel was removed perpendicular to the growth axis of each tooth every 2–3 mm using a low-speed dental drill. The number of samples collected from each specimen depended on specimen size and enamel quality and ranged from 2–5 for each litoptern, 3–6 for each hegetotheriid, and 6–8 for each toxodontid. In total, 92 samples were analyzed. Powdered samples were treated with a 3% hydrogen peroxide solution followed by 0.1 M acetic acid to remove surficial carbonates and to ensure that only biological material was analyzed. The powdered enamel was reacted with 100% phosphoric acid, and the resulting CO_2 was analyzed on a dual-inlet isotope ratio mass spectrometer.

We calculated a separate apparent diet-bioapatite (enamel) enrichment factor (ε*) for each species using its body mass and the average linear regression equation for hindgut fermenters of Tejada-Lara et al. (2018: table 2a). Below, we compare our new data to carbon isotope data from Oligocene and Miocene notoungulates and astrapotheres from Bolivia published by MacFadden et al. (1994) and Bershaw et al. (2010) and from Early Miocene astrapotheres from Argentina published by MacFadden et al. (1996). We recalculated published values using body-mass-specific enrichment factors (rather than the ε* values of 13‰ or 14‰ used in these works) to permit direct comparisons among datasets. Most SANU body mass estimates were based on Nelson et al. (2023) or Cassini et al. (2012) or were calculated using regression equations from Damuth and MacFadden (1990). Body mass estimates, species-specific enrichment values, and taxonomic updates to published identifications are provided in SOM 1 (Supplementary Online Material available at http://app.pan.pl/SOM/app70-VanOrman_etal_SOM.pdf).

Geographic, geological, and paleoenvironmental setting

The Quebrada Honda Basin (QHB) is situated in the Eastern Cordillera of the Andes Mountains in the Department of Tarija in southern Bolivia (Figs. 1, 2). Late Middle Miocene fossils have been collected from this site since the 1970s, including nearly 40 species of mammals in addition to birds and reptiles (e.g., Hoffstetter 1977; MacFadden and Wolff 1981; Frailey 1987, 1988; Villarroel and Marshall 1988; MacFadden et al. 1990; Sánchez-Villagra et al. 2000; Goin et al. 2003; Croft and Anaya 2006; Forasiepi et al. 2006; Croft 2007; Croft et al. 2011; Pujos et al. 2011, 2014; Engelman and Croft 2014; Engelman et al. 2017, 2020; Brandoni et al. 2018; McGrath et al. 2018, 2020; Strömberg et al. 2024). Today, the area is at > 3,500 m above sea level, but paleontological and geological evidence suggest that it may have been ≤1,000 m when its fossils were preserved (Cadena et al. 2015; Saylor et al. 2022).

Studies of QHB paleosols, ichnofossils, and mammal ecological diversity analysis have concluded that the basin infill records a seasonal, sub-humid to semi-arid wooded grassland or savanna-like environment with mean annual precipitation around 1,000 mm (Catena et al. 2017; Catena and Croft 2020). A recent study of QHB plant silica (phytolith) data (Strömberg et al. 2024) recognized two broad types of vegetation associations within the QHB: one with many presumably open-habitat grasses that likely represents an open habitat, and another with more forest indicators and possible bamboos that likely represents a more closed habitat. Based on the taxonomic overlap between these associations, the lack clear spatial or temporal variation patterns in their presence, and the absence of clear geographic or temporal difference in mammal abundances, these authors concluded that these plant communities were part of a single biome. This biome likely has no close modern analog but represents a warm habitat with seasonal precipitation that was partially to predominantly wooded (Strömberg et al. 2024).

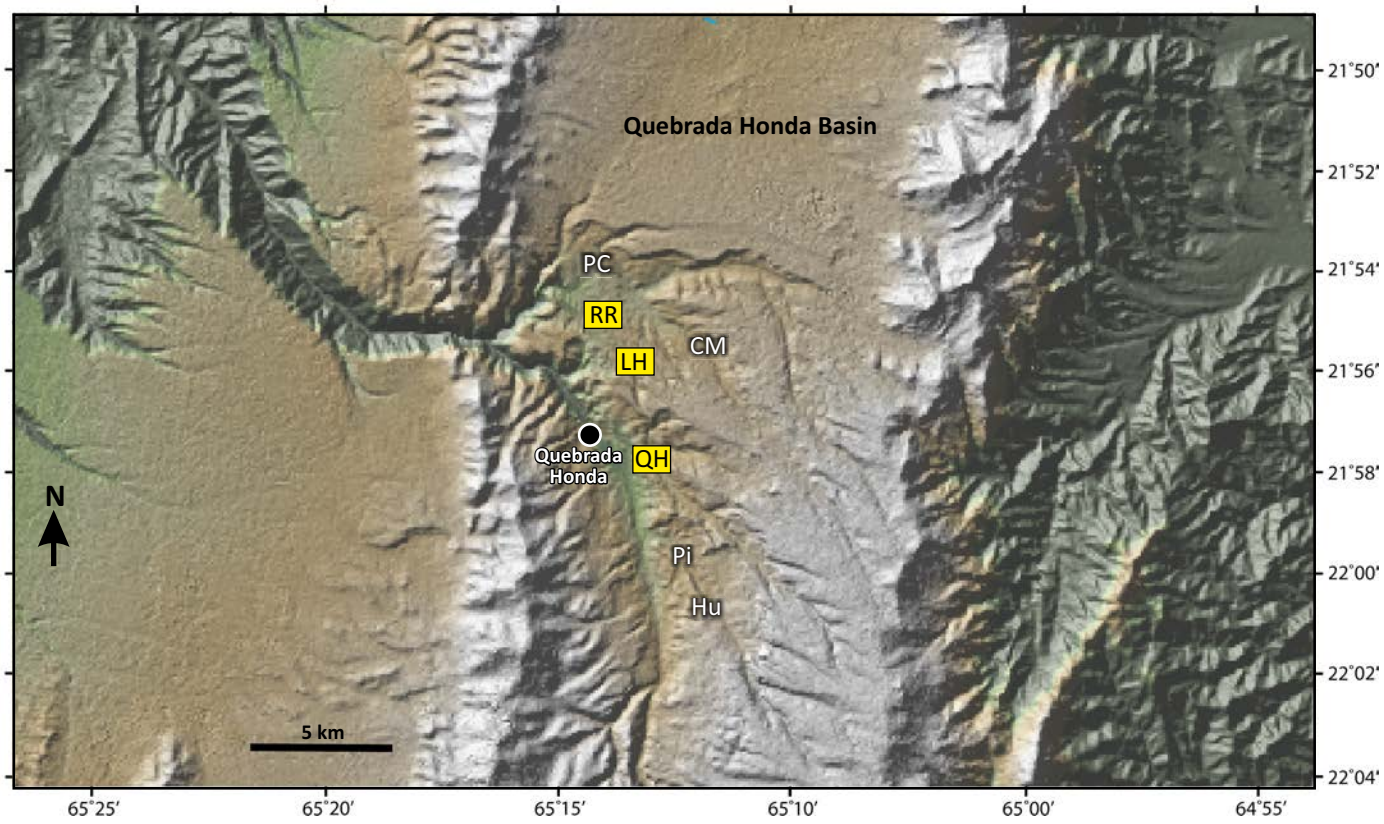

Fig. 2. Shaded relief map showing collecting areas of the Quebrada Honda Basin (QHB). The ones highlighted in yellow have yielded astrapothere remains and include Río Rosario (RR), La Hoyadita (LH), and Quebrada Honda (QH). From north to south, other recognized local areas include Papa Chacra (PC), Casa del Ministro (CM), Pisa (Pi), and Huayllajara (Hu). Image modified from Strömberg et al. (2024: fig. 1).

Two recent works (Gibert et al. 2020 and Saylor et al. 2022) have detailed the geochronology and sedimentology of the Middle Miocene sediments of the QHB, which are exposed across > 50 km^2 of plateau, tributary margins, and slump blocks. Geological and paleontological studies have focused on six areas within the basin: Quebrada Honda, Rio Rosario, Huayllajara, Papa Chacra, Casa del Ministro, and Pisa. The Quebrada Honda and Río Rosario local areas have produced more than 80% of QHB vertebrate fossils (Strömberg et al. 2024) and have long been the focus of QHB research.

The sediments of the QHB have yet to receive formal designation but are mapped as belonging to the Honda Group (MacFadden et al. 1990; Gibert et al. 2020). The composite section is nearly 200 m thick and consists mainly of pedogenically-altered mudstones with intervals of sandstone, conglomerate, pedogenic carbonate, and volcanic tuff (Saylor et al. 2022). Three widespread lithostratigraphic units are recognized above a basal breccia; from lowest to highest, they are units A, B, and C (Fig. 3). Unit A, which mainly consists of pedogenically modified mudstones and intervals of pedogenic carbonate, is divided into sub-units A-lower, A-middle, and A-upper. Most fossils (nearly 80%) derive from sub-unit A-lower (Strömberg et al. 2024). The middle unit, Unit B, is slightly fossiliferous and characterized by intervals of pedogenic carbonate that are coalesced into calcrete (MacFadden and Wolff 1981; Saylor et al. 2022). It is divided into sub-units B-lower and B-upper. Unit C, which is difficult to access and has yielded few fossils, consists of red beds and conglomerates.

Systematic paleontology

Class Mammalia Linnaeus, 1758
Order Astrapotheria Lydekker, 1894
Family Astrapotheriidae Ameghino, 1887
Subfamily Uruguaytheriinae Kraglievich, 1928
Uruguaytheriinae gen.? et sp. nov.

Figs. 4–9.

Material.—UATF-V-002013, partial left maxilla bearing DP2–3 and an associated deciduous lower incisor; MNHN. F.BLV 46, many tooth and bone fragments, including a mostly complete left m3 and large fragments of right m3 and both M3s; MNHN-BOL-V-003672, partial rostrum preserving left and right DP2-4; UF 26679, partial posterior cranium and fragments of upper cheek teeth, including mesiobuccal fragments of both M3s; UF 563068, several upper molar and enamel fragments.

The astrapothere specimens described herein were collected from the Quebrada Honda and Río Rosario local areas

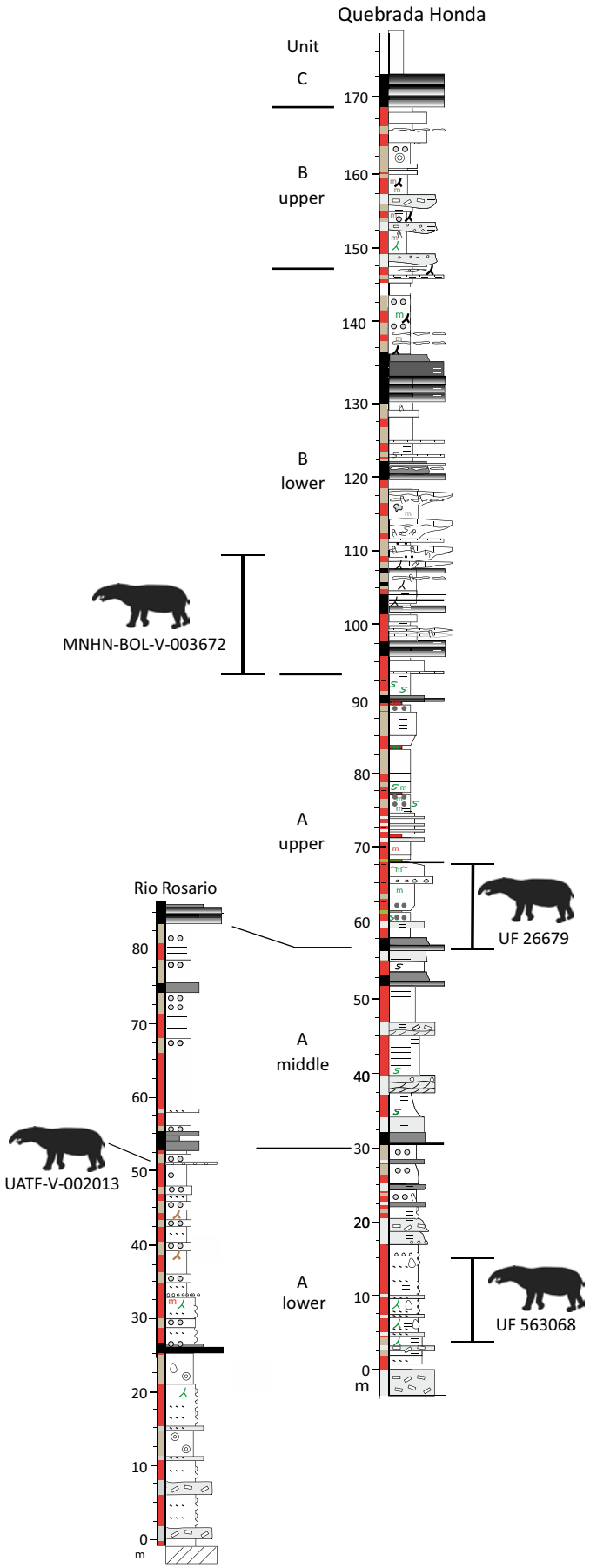

of the QHB (see Gibert et al. 2020; Saylor et al. 2022) plus a third area approximately midway between them known as "La Hoyadita" (Fig. 2).

UATF-V-002013 was collected from the top of sub-unit A-lower at Rio Rosario, just below tuff *RR53 (Fig. 3). Saylor et al. (2022) correlated this interval to paleomagnetic chron C5Ar.3r based on the local paleomagnetic section and dated tuffs from MacFadden et al. (1990) and Gibert et al. (2020), indicating an age of 13.032–12.887 Ma (Ogg 2012).

MNHN.F.BLV 46 was collected by Robert Hoffstetter and was the basis for his report of astrapotheres at Quebrada Honda (Hoffstetter 1977). In that work, he mentions that the specimen was collected 1.2 km east of the town of Quebrada Honda, presumably in deposits corresponding to what is recognized today as the Quebrada Honda Local Area. However, no field notes are present at the MNHN-Paris that might provide additional details about its exact geographic or stratigraphic position (Guillaume Billet, personal communication 2024).

MNHN-BOL-V-003672 was collected in 1994 from "La Hoyadita," an area between the Quebrada Honda and Rio Rosario local areas. These outcrops appear to correlate with the lower half of sub-unit B-lower (Fig. 3) based on satellite imagery, but we have not had the opportunity to investigate these outcrops firsthand. If correct, this suggests an age of 12.735–12.474 Ma for the specimen, following Saylor et al. (2022) and assuming a correlation to chron C5Ar.1r (Ogg 2012). To our knowledge, no other fossil specimens have been collected from this site.

UF 26679 was collected in 1978 from unit 3 of section 2 of MacFadden and Wolff (1981) at the Quebrada Honda Local Area (Fig. 3). The exact stratigraphic position of the specimen was indicated by Frailey (1987: fig. 1) and corresponds to local magnetic polarity zone N2 of MacFadden et al. (1990: fig. 4). This interval pertains to sub-unit A-upper and correlates to C5Ar.2n of the Geomagnetic Polarity Timescale (MacFadden et al. 1990; Gibert et al. 2020; Saylor et al. 2022), indicating an age of 12.887–12.829 Ma (Ogg 2012).

UF 563068 was collected from unit 2 of section 1 of MacFadden and Wolff (1981), the lowest fossil-yielding level at the Quebrada Honda Local Area (Fig. 3). This level spans local magnetic polarity zone N1 of MacFadden et al. (1990: fig. 4) as well as a lower reversed polarity zone (R0) subsequently recognized by Saylor et al. (2022). Saylor et al. (2022) correlated these local magnetic polarity zones to C5AAr and C5AAn of the Geomagnetic Polarity Timescale (Saylor et al. 2022: fig. 4), which span 13.363–13.032 Ma (Ogg 2012).

Fig. 3. Composite stratigraphic sections for the Río Rosario and Quebrada Honda local areas showing boundaries between the six main lithostratigraphic units recognized by Gibert et al. (2020) and Saylor et al. (2022) and stratigraphic positions of astrapothere specimens. Astrapothere silhouette (*Hilarcotherium miyou*) is by Zimices from Phylopic.org (CC BY-NC-3.0). Modified from Saylor et al. (2022: fig. 3).

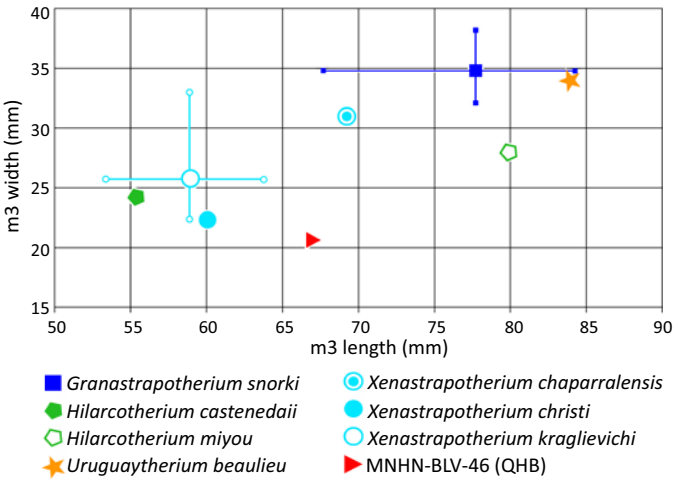

Fig. 4. Plot of m3 length and width for late Oligocene and Miocene astrapotheres, including MNHN.F.BLV 46 from the QHB. Measurements and sources are listed in SOM 2.

Diagnosis.—Member of the Uruguaytheriinae based on the presence of an oblique paraflexid in m3 (Ch. 28:1 of Kramarz et al. 2019). Shares widely flaring zygomatic arches (see Frailey 1987) with the uruguaytheriines *Granastrapotherium snorki* Johnson & Madden, 1997, and *Hilarcotherium castanedaii* Vallejo-Pareja et al., 2015 (otherwise known to be present only in late Eocene *Astraponotus*; Ch. 54:1 of Kramarz et al. 2019). Differs from *Granastrapotherium snorki* in size (~15% smaller based on m3 length; Fig. 4; see also SOM 2) and likely the presence of permanent lower incisors (*G. snorki* lacks lower incisors; Johnson and Madden 1997; Croft et al. 2020b; see discussion below). Differs from *Hilarcotherium castanedaii* in size (~15% larger based on m3 length). Likely further differs from both *G. snorki* and *H. castanedaii* in having two permanent upper premolars (rather than just one; see discussion below). Differs from *Hilarcotherium miyou* Carrillo et al., 2018, in presence of a M3 central valley that is open lingually (Ch. 37:0 of Kramarz et al. 2019), the absence of hypoflexid in m3, and size (~15% smaller based on m3 length). Differs from *Uruguaytherium beaulieui* Kraglievich, 1928, in the absence of a transverse paraflexid in m3 and size (~20% smaller based on m3 length). Differs from *Xenastrapotherium christi* Stehlin, 1928, in the absence of a hypoflexid on m3 and size (~10% larger based on m3 length). Differs from *Xenastrapotherium kraglievichi* Cabrera, 1929, in size (~10–15% larger based on m3 length), greater unilateral hypsodonty in deciduous teeth (described below), presence of a M3 central valley that is open lingually, and perhaps absence of hypoflexid on m3 (this is variable in *X. kraglievichi*; Johnson and Madden 1997: 357; Kramarz et al. 2019). Differs from *Xenastrapotherium aequatorialis* Johnson & Madden, 1997, in lacking an internal talonid pillar fused to the metalophid and likely size (*X. aequatorialis* is similar in size to *X. kraglievichi*; Johnson and Madden 1997: 363). Differs from *Xenastrapotherium amazonense* (Paula Couto, 1979) in presence of a M3 central valley that is open lingually and size (*X. amazonense* is comparable to *G. snorki* in size; Johnson and Madden 1997: tables 22.3, 22.4). Differs from *X. chaparralensis* in presence of a M3 central valley that is open lingually and absence of hypoflexid in m3 (it is weakly developed in *Xenastrapotherium chaparralensis* Johnson & Madden, 1997; Johnson and Madden 1997), and perhaps lower molar proportions (see below).

Remarks.—We conservatively refer all QHB specimens to a single species because no evidence suggests that more than one species may be present at the site; all specimens are similar in size (see discussion below), and no discrete morphological features suggest referral to more than one taxon is warranted. Taxonomic differences in other QHB mammal groups have not been documented through the stratigraphic section or in different parts of the basin (Strömberg et al. 2024), indicating there is no a priori reason to favor a multi-species interpretation over a single-species interpretation.

Precise identification of the astrapothere remains from the QHB are hampered by a variety of factors including the limited dental remains available from the QHB, little information about the deciduous teeth of other uruguaytheriines (especially DP2–3 and deciduous lower incisors), the very limited remains on which several *Xenastrapotherium* species are based (three species have never been included in a phylogenetic analysis; see Carrillo et al. 2018; Kramarz et al. 2019), and the small number of apomorphies that distinguish uruguaytheriine species from one another. In addition, the monophyly of both *Xenastrapotherium* and *Hilarcotherium* is unclear; no phylogenetic analysis has provided strong evidence that the species presently included in these genera share a more recent common ancestor with one another than with other uruguaytheriines (Carrillo et al. 2018: fig. 12; Kramarz et al. 2019: fig. 4).

In the above context, one of the clearest indications that the QHB astrapothere represents a distinct uruguaytheriine species is its size; based on m3 length (Fig. 4), it is larger than *H. castanedaii*, *X. christi*, *X. kraglievichi*, and *X. aequatorialis* and smaller than *G. snorki*, *H. miyou*, *U. beaulieui*, and *X. amazonense*. Notably, it falls in the size gap between the two well-documented species from the contemporaneous site of La Venta, *X. kraglievichi* and *G. snorki* and (Fig. 4). The observation that the QHB astrapothere is intermediate in size compared to most other uruguaytheriines based on m3 length is compatible with Frailey's (1987) inference that it was similar in size to *Astrapotherium magnum* (Owen, 1853); *A. magnum* is ~10% larger than *X. kraglievichi* based on molar row length (Kramarz and Bond 2011: table 3), similar to the inferred size difference between the QHB species and *X. kraglievichi* based on m3 length (~15% larger).

Among named uruguaytheriines, *X. chaparralensis* may be closest in size to the QHB astrapothere based on m3 length, being only ~5% larger. However, the single known m3 of this species is about 50% broader. Part of this difference likely reflects the nearly unworn state of the QHB specimen and its incomplete preservation (see Description, below), but Johnson and Madden (1997) highlighted greater lower molar area (i.e., broader molars) as a distinguishing

feature of *X. chaparralensis*; thus, part of this difference may be taxonomically significant. Regardless, the QHB species differs from *X. chaparralensis* in the absence of a hypoflexid. The QHB species differs or likely differs from all other uruguaytheriines in at least one discrete morphological character.

The number of permanent upper premolars in the QHB species is not known. A common pattern in Oligocene and Miocene astrapotheres is that three deciduous upper premolars are succeeded by only two permanent upper premolars; for example, this occurs in *Parastrapotherium* spp. (Kramarz and Bond 2008), *Astrapothericulus iheringi* (Ameghino, 1899) (Kramarz 2009), and probably also in *Astrapotherium magnum* (Scott 1928; Alejandro Kramarz, personal communication 2025). However, the number of deciduous upper premolars in species with only a single permanent upper premolar (i.e., *Comahuetherium coccaorum* Kramarz & Bond, 2011, *Astrapotherium guillei* Kramarz et al., 2019, *G. snorki*, and *H. castanedaii*) has not yet been documented. If these species are characterized by two or fewer deciduous upper premolars, this would be an additional feature that distinguishes them from the QHB species.

Among other placental mammals, we are unaware of any taxon with well-developed cheek teeth in which the numbers of deciduous and permanent premolars differ by more than one. For example, juvenile mesotheriine notoungulates have DP2–4/dp3–4, and adults have P3–4/p4 (Francis 1965; but see Cerdeño and Schmidt 2013 for a different interpretation). Similarly, the extant hyracoid *Procavia capensis* (Pallas, 1766) has dp1–4 and p2–4 (Asher et al. 2017), and an undetermined species of the extinct pyrothere genus *Pyrotherium* Ameghino, 1888, has dp2–4 and p3–4 (Folino et al. 2024). The extant aye aye, *Daubentonia madagascariensis* Gmelin, 1788, has dp3–4 and no permanent lower premolars, but its cheek teeth are highly simplified (Ankel-Simons 1996). These observations suggest that P3–4 were likely present in an adult QHB astrapothere. If true, this precludes referral to *Granastrapotherium* or *Hilarcotherium* (or at least to *H. castanedaii*, the genotypic species).

The presence of a lower deciduous incisor in the QHB species casts further doubt on referral to *Granastrapotherium*. It is possible that lower incisors were only absent in adults of *Granastrapotherium*, but we are unaware of any mammals in which fully developed deciduous lower incisors are present in juveniles and absent in adults. As for premolars, the number of deciduous and permanent incisors may differ by one; this has been documented for upper incisors in the extant afrosoricidan *Tenrec ecaudatus* (Schreber, 1777) (Butler 1937) and for lower incisors in *Pyrotherium* sp. (Folino et al. 2024). The QHB astrapothere likely cannot be referred to *Uruguaytherium*, a taxon that is distinguished from the QHB species and other uruguaytheriines by its transverse lower molar paraflexid.

Whether the QHB astrapothere can be (or at least should be) referred to *Xenastrapotherium* is less clear but also seems unlikely. The genus is based on *Xenastrapotherium christi*, which is known only from the holotype: a partial mandible bearing p4–m3 and partial alveoli of the anterior dentition (Stehlin 1928; Carrillo et al. 2018). The only other well-characterized species is *X. kraglievichi* from La Venta, which is known from multiple specimens representing the entire adult dentition (Cabrera 1929; Johnson and Madden 1997). None of the three remaining *Xenastrapotherium* species is known from much more than limited dental specimens: *Xenastrapotherium aequatorialis* is based on a dentary in several pieces with nearly complete m1–2 (Johnson and Madden 1997); *Xenastrapotherium amazonense* is represented by a maxillary fragment bearing a nearly complete M3 (the holotype), three referred specimens (including a P3) and three lower molar fragments (Paula Couto 1976), plus four possible lower teeth, including three molars and a canine (Ranzi 2008); and the holotype of *X. chaparralensis* consists of half a dozen associated teeth, some incomplete (Stirton 1947).

The emended diagnosis of *Xenastrapotherium* by Johnson and Madden (1997: 357) lists five features: (i) two pairs of lower incisors; (ii) posterolingual cingulum on M3 that joins the protoloph with the metaloph and closes the median (central) valley lingually; (iii) lower canine tusks with pronounced longitudinal curvature and anteroinferior and posteroinferior grooves in cross section; (iv) shallow lower molar metaflexids (= paraflexids) bounded by a variably developed anterolingual cingulum; and (v) mesiodistally narrow and rounded metalophids. Of these, only three can be assessed in the genotypic species, *X. christi* (number of lower incisors and two lower molar features). Among these three features, shallow lower molar paraflexids are not unique to *Xenastrapotherium* (they also characterize *Granastrapotherium* and *Hilarcotherium*; see Kramarz et al. 2019: Ch. 28), and the taxonomic utility of the shape and proportions of the metalophid is unclear; no such character has been incorporated into subsequent phylogenetic analyses or used in diagnoses of other species or genera (e.g., Vallejo-Pareja et al. 2015; Carrillo et al. 2018; Kramarz et al. 2019). The presence of a posterolingual cingulum on M3 does distinguish *X. kraglievichi* (and *X. amazonense*) from *G. snorki*, but it cannot presently be coded for most other uruguaytheriines (including other species to *Xenastrapotherium*). This feature is present in the QHB astrapothere (see description of MNHN.F.BOL.46 below), which precludes referral to *X. kraglievichi*. The number of lower incisors is known (or reasonably inferred) for *X. christi* and *X. kraglievichi* but not the other three species referred to *Xenastrapotherium*. In summary, even though some species referred to *Xenastrapotherium* preserve unique combinations of character states, no adequate diagnosis exists for the genus or even a clade that encompasses multiple *Xenastrapotherium* species. Given this context and the differences between the QHB species and the best-characterized species of *Xenastrapotherium* (*X. kraglievichi*; see below), there is no evidence to suggest referral to this genus.

UATF-V-001981 from Cerdas, Bolivia was identified as a new species of uruguaytheriine that could represent a distinct

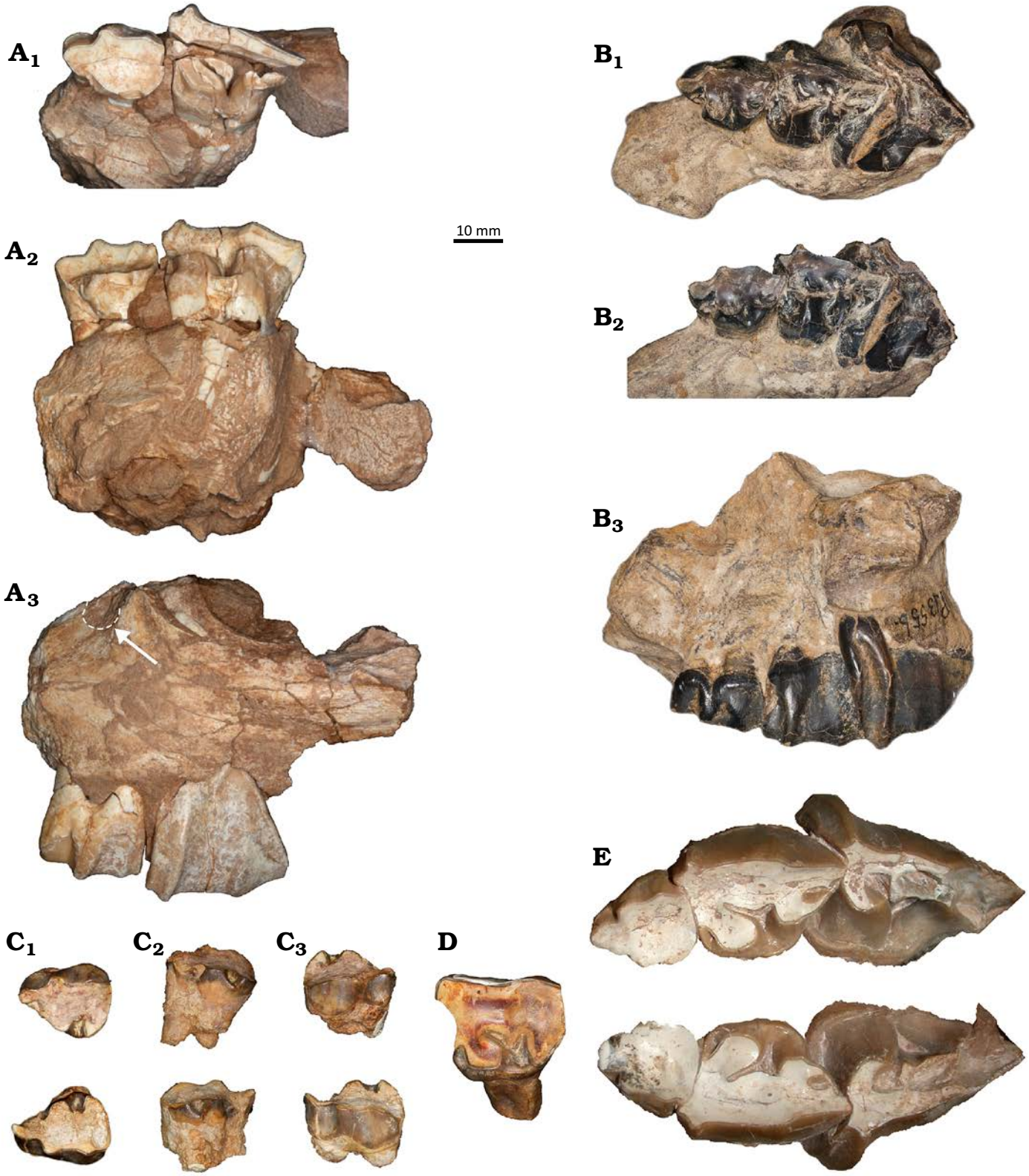

Fig. 5. Astrapothere upper deciduous premolars. **A**. UATF-V-002013, Uruguaytheriinae gen.? et sp. nov. (upper Middle Miocene, QHB, Bolivia), left DP2–3 in occlusal (A_1), lingual (A_2), and buccal (A_3) views; the white arrow and dashed line in in A_3 indicate the inferior border of the infraorbital foramen. **B**. FMNH PM 13556, *Parastrapotherium holmbergi?* Ameghino, 1895 (upper Oligocene, La Flecha, Santa Cruz, Argentina), left DP2–4 in occlusal (B_1), lingual (B_2), and buccal (B_3) views. **C**, **D**. IGM-2061-F, *Xenastrapotherium kraglievichi* Cabrera, 1929 (upper Middle Miocene, La Venta, Colombia). **C**. Left DP2 (top) and right DP2 (bottom) in occlusal (C_1), lingual (C_2), and buccal (C3) views. **D**. Left DP3 in occlusal view. **E**. MNHN-BOL-V-003672, Uruguaytheriinae gen.? et sp. nov. (upper Middle Miocene, QHB, Bolivia), left and right DP2–4 in occlusal view. Anterior is to the left in all images except the upper right and lower center images in C.

genus (Croft et al. 2016). Although this material is fragmentary (it primarily includes parts of upper cheek teeth; Croft et al. 2016), the remains have characteristics unique among astrapotheres. For example, the M1 of the Cerdas astrapothere has an anterolingual pocket that is much larger than in any other uruguaytheriine. Additionally, a small fossette at the intersection of the metaloph and ectoloph on the M1 or M2 has not been observed in any other astrapothere. No direct comparison can be made between the material from the QHB and Cerdas. However, the QHB species is ~10–15% larger than *X. kraglievichi* based on m3 length, whereas the Cerdas species is ~30% larger than *X. kraglievichi* based on P4 length (Croft et al. 2016: fig. 7C, D). This suggests that the QHB species is ~10–15% smaller than the Cerdas species. Although the two are unlikely to represent the same species based on this size difference, we presently cannot rule out the possibility that they pertain to the same undefined (potentially new) genus. Relatively few genera or species of QHB mammals are shared with Cerdas, but they do include two SANUs: the mesotheriid notoungulate "*Plesiotypotherium*" *minus* Villarroel, 1978, and the litoptern *Llullataruca shockeyi* McGrath et al., 2018 (Townsend and Croft 2010; McGrath et al. 2018; Strömberg et al. 2024). Assessing whether they share an astrapothere genus or species will require additional remains from both sites.

The two lower molar specimens from Nazareno are fragmentary (SOM 3), but one of them (UATF-V-001054) appears to lack a well-defined hypoflexid. We tentatively refer the Nazareno material to the Uruguaytheriinae for this reason, but a more specific identification is not possible.

Description.—UATF-V-002013 consists of a partial left maxilla with DP2–3, part of the alveolus of DP4, and an associated deciduous lower incisor (Fig. 5A; a 3D mesh also available on MorphoSource: https://www.morphosource.org). The maxillary specimen preserves a small portion of the orbital rim as well as much of the inferior portion of the infraorbital foramen (Fig. 5A, bottom). The foramen measures 8.9 mm in mediolateral diameter (it lacks a roof) and is oriented ca. 45° to the sagittal plane in dorsal view. We identify the teeth preserved in UATF-V-002013 as DP2–3 based on their similar sizes, occlusal outlines, and general morphologies to homologous teeth of *Astrapotherium* spp. (Ameghino 1904: fig. 117; Kramarz et al. 2019: supp. data S1: fig. 2) and *Parastrapotherium* spp. (e.g., FMNH PM 13556; Scott 1937; see also below). They also compare closely with the two most mesial teeth in MNHN-BOL-V-003672, a partial rostrum that includes the palate and what we interpret as left and right DP2–4 (this last tooth is in eruption; Fig. 5D).

Relatively few deciduous teeth have been described for late-diverging astrapotheres, particularly DP2 and DP3 (the best-preserved loci in our specimens), which limits comparisons to the astrapotheriines *Parastrapotherium* and *Astrapotherium*. However, IGM-2061-F, a specimen collected from the Villavieja Formation at La Venta, Colombia, includes left and right DP2 and a left DP3; these are associated with partial left and right maxillary and mandibular den-

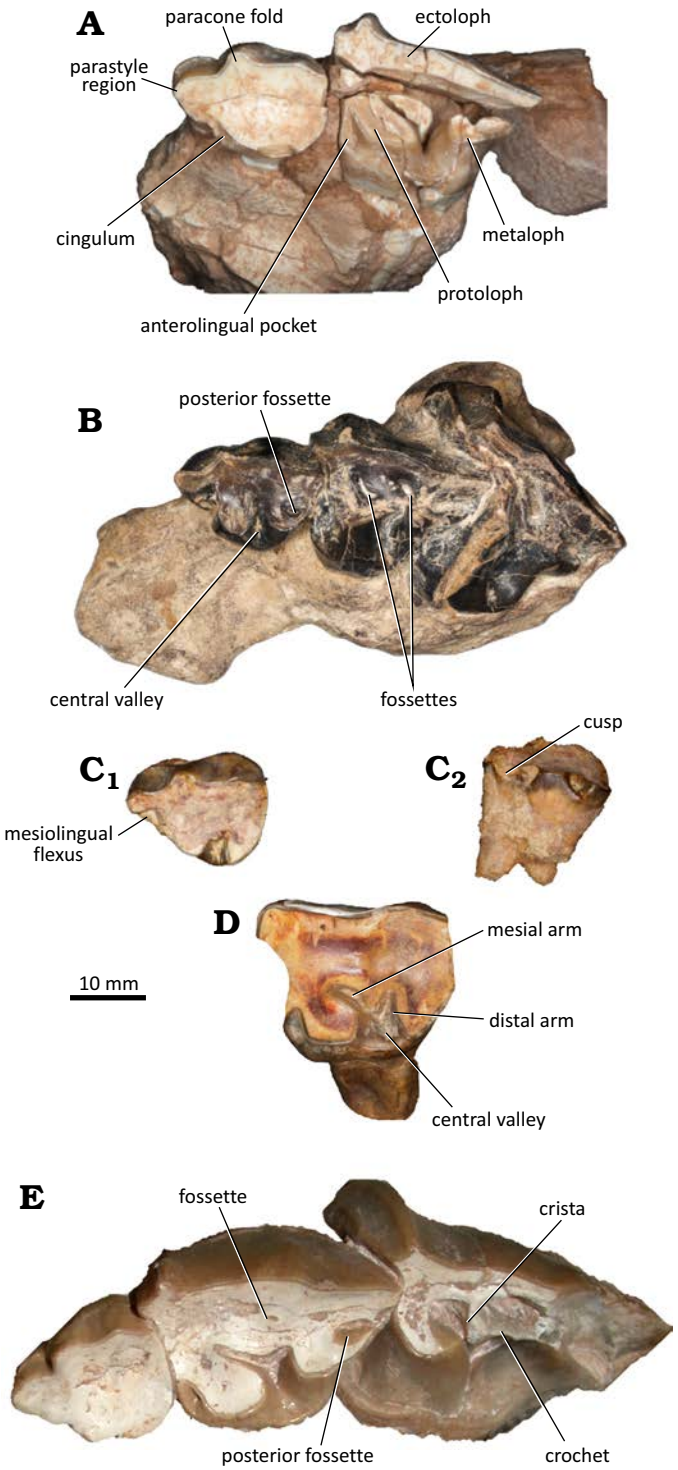

Fig. 6. Astrapothere upper deciduous premolars from Fig. 5, labeled with structures discussed in text. **A**. UATF-V-002013, Uruguaytheriinae gen.? et sp. nov. (upper Middle Miocene, QHB, Bolivia), left DP2–3 in occlusal view. **B**. FMNH PM 13556, *Parastrapotherium holmbergi?* Ameghino, 1895 (upper Oligocene, La Flecha, Santa Cruz, Argentina), left DP2–4 in occlusal view. **C**, **D**. IGM-2061-F, *Xenastrapotherium kraglievichi* Cabrera, 1929 (upper Middle Miocene, La Venta, Colombia). **C**. Left DP2 in occlusal (C_1) and lingual (C_2) view. **D**. Left DP3 in occlusal view. **E**. MNHN-BOL-V-003672, Uruguaytheriinae gen.? et sp. nov. (upper Middle Miocene, QHB, Bolivia), left DP2–4 in occlusal view. Anterior is to the left in all images.

titions that preserve recently-erupted upper and lower first molars and fragments of additional deciduous premolars. The specimen label refers the material to *Xenastrapotherium* sp., and we agree with this identification based on the presence of a lingual cingulum in M3, a feature absent in the other common astrapothere of La Venta, *G. snorki* (Johnson and Madden 1997; Croft et al. 2020b). The other astrapothere of similar age from Colombia, *H. castanedaii*, has not yet been reported from the Villavieja Formation (only the La Victoria Formation). Additionally, IGM-2061-F is ca. 20% larger than *H. castanedaii* based on m1 length (ca. 43 mm vs. 36 mm, respectively; DAC personal observation and Vallejo-Pareja et al. 2015: appendix 2). The well-preserved deciduous premolars of IGM-2061-F are illustrated here for the first time (Fig. 5C).

Parastrapotherium is known from many adult specimens and some juvenile specimens that preserve deciduous teeth. FMNH PM 13556, which preserves DP2–4 (Fig. 5B), was described by Scott (1937) and is included in our comparisons. Deciduous premolars have been mentioned for *Astrapotherium* sp. (e.g., Ameghino 1904; Scott 1928), but we have not been able to study any firsthand. Kramarz et al. (2019) recently identified the holotype of *Astrapotherium delimitatum* (Ameghino, 1902) (= *Astrapotherium burmeisteri* Mercerat, 1891) as a DP2, and we include information from that specimen (MACN-A 3299) and a presumably associated DP4 noted by the same authors (MACN-A 3300) in our comparisons.

A conspicuous feature of the deciduous premolars of the QHB astrapothere is that they are more hypsodont than those of other astrapotheres (Fig. 5). The DP2 of UATF-V-002013 is quite worn, with a smooth occlusal surface and no sign of a hypoflexus or fossettes (Fig. 6A). The height of the ectoloph is ~17 mm from the base of the enamel to the occlusal surface (excluding cusps and measured perpendicular to the occlusal surface). The ectoloph of the slightly less worn DP3 is ~32 mm tall. Deciduous premolars of IGM-2061-F (*X. kraglievichi*) appear less worn than those of UATF-V-002013 from the QHB; both DP2 and DP3 retain the lingual portion of the hypoflexus, and both branches of the central valley are evident in DP3 (Fig. 6C, D). Nevertheless, the ectoloph of DP2 is only ~8 mm tall (we lack data for DP3), about half the height of the corresponding tooth of UATF-V-002013 despite its similar occlusal dimensions (Fig. 7; SOM 2). Deciduous premolars of FMNH PM 13556 (*Parastrapotherium* sp.) appear less worn than those of the available uruguaytheriine specimens; the DP2 preserves a prominent mesiolingual flexus and a distal fossette in addition to a prominent central valley, and the DP3 is not fully erupted (the distal portion is unworn; Fig. 6B). The ectoloph of DP2 is ~11 mm tall, two-thirds the height of UATF-V-2013, whereas that of DP3 is ~20 mm, less than two-thirds that of UATF-V-002013. The DP2 of *A. burmeisteri* (MACN-A 3299) appears to be less worn than those of the QHB astrapothere but more worn that than of *Parastrapotherium*; the central valley and a mesiolingual flexus are evident, but no fossettes are preserved (Kramarz et al. 2019: supp. data S1: fig. 2). The central valley appears to be relatively deeper than that of *Parastrapotherium*, reflecting the greater hypsodonty of *Astrapotherium* compared to *Parastrapotherium* (Kramarz and Bond 2008). The ectoloph of MACN-A 3299 measures ~7 mm, about 40% of the corresponding height of the QHB astrapothere (UATF-V-002013); the two specimens are equal in length (Fig. 7; SOM 2), indicating much greater hypsodonty in the QHB species.

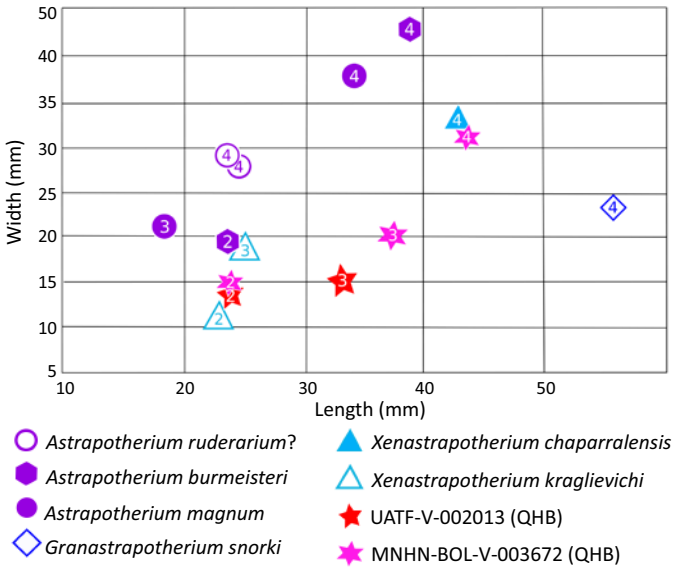

Fig. 7. Plot upper deciduous premolar dimensions (DP2–4) for Miocene astrapotheres. The number in each symbol indicates the DP locus. Measurements and sources are listed in SOM 2.

The crown of DP2 of UATF-V-002013 is complete except for a small portion of the mesiolingual surface. In occlusal view (Fig. 6A), it is subtriangular due to the anterior projection of the parastyle into a distinct lobe. The parastyle region makes up about a third of its mesiodistal length and about half of its buccolingual breadth. Vertical folds of the paracone and metacone are pronounced on its buccal wall. The paracone fold projects perpendicularly and is about half as broad mesiodistally as the parastyle is buccolingually. In the more worn DP2 of MNHN-BOL-V-003672 (Fig. 6E), the parastyle forms a distinct lobe but is more rounded and broader buccolingually; the paracone fold is wider and less salient than in UATF-V-002013. The paracone fold is smaller in *Parastrapotherium* sp. (Fig. 6B) and *A. burmeisteri* (Kramarz et al. 2019: supp. data S1: fig. 2) than in the QHB astrapothere but is similarly developed in *X. kraglievichi* (Fig. 6C). The paracone fold of *X. kraglievichi* is slightly more rounded than that of UATF-V-002013. In UATF-V-002013, the metacone fold is much less pronounced than the paracone fold, and the buccal face distal to it is relatively flat. The lingual side of DP2 is rounded, with no obvious distinction between protocone and hypocone (i.e., no sign of a central valley or hypoflexus). The distal face is relatively flat and does not overlap the DP3, a wear-related condition also evident in MNHN-BOL-003672 and IGM-2061-F (*X. kraglievichi*). In FMNH

PM 13556 (*Parastrapotherium* sp.), the buccodistal corner of DP2 overlaps the mesial face of DP3.

In lingual view (Fig. 5A, middle), the buccal wall of the DP2 of UATF-V-002013 is much taller than the lingual wall, illustrating its unilateral hypsodonty. The paracone fold marks the point of greatest relief of the occlusal surface. A similar condition is present in *Parastrapotherium* sp. and apparently in *A. burmeisteri,* but in *X. kraglievichi*, the buccal wall is only slightly higher than the lingual wall. A small cingulum on the anterolingual wall of the DP2 of UATF-V-002013 that intersects the base of the parastyle likely represents the remnants of the anterolingual flexus present in *X. kraglievichi*, *Parastrapotherium* sp., and *A. burmeisteri*. In *X. kraglievichi*, a small, rounded cusp is present in this region between the protocone and the parastyle (Fig. 5C, center); this feature is not present in *X. kraglievichi* or *Parastrapotherium* sp. In *A. burmeisteri*, a relatively long, narrow lobe extends lingually from the occlusal surface in this region and may represent the same structure.

In buccal view, a cingulum extends the length of UATV-V-002013 but blends with the base of the metacone fold (Fig. 5A, bottom). At its mesial terminus, it rises towards the parastyle but terminates before it reaches the occlusal surface. At its distal terminus, it rises to meet the occlusal surface of the metastyle. A similar condition is present in *Parastrapotherium* sp. but is difficult to discern in *X. kraglievichi.*

The DP3 of UATF-V-002013 is fractured and missing a large portion of the occlusal surface lingual to the ectoloph. It is subtriangular in occlusal view (Fig. 6A), with a broad mesial face and a pointed distal face, though this face is partly obscured by the fracture. The subtriangular outline of DP3 is clearer in MNHN-BOL-V-003672 (Fig. 6E). The DP3 of *Parastrapotherium* sp. is similar in overall form (Fig. 6B), whereas the DP3 of *X. kraglievichi* is subquadrangular due to its much greater wear and pronounced interdental facets (Fig. 4D). The parastyle is small but well demarcated in the DP3 of UATF-V-002013. It primarily extends in a mesial direction and is slightly smaller than the paracone fold. The paracone fold is well pronounced and mesiodistally narrow. In MNHN-BOL-V-003672, these structures are similar but more rounded and slightly less pronounced due to greater wear. They have been completely worn away in the *X. kraglievichi* specimen. In *Parastrapotherium* sp., the parastyle is more pronounced than in UATF-V-002013 and extends further anteriorly. The paracone fold in *Parastrapotherium* sp. is similar to that of UATF-V-002013. However, in buccal view (Fig. 5B, bottom) it broadens toward the base of the tooth, a condition not evident in the QHB astrapothere (Fig. 5A, bottom). No buccal cingulum is present in UATF-V-002013, and no distinct metacone fold is present in any of the available DP3s.

In occlusal view, the protoloph of the DP3 of UATF-V-002013 extends distolingually from the ectoloph. Its lingual terminus is broad and directed distally and has lingual and buccal walls that are roughly parallel to one another. The metaloph is about half as long as the protoloph but is missing its central portion. The protoloph and metaloph are separated by the lingual portion of the central valley; the rest of the central valley is not preserved. In MNHN-BOL-V-003672, the mesial branch of the central valley is much longer than the distal branch, and the two are separated by a small, rounded crista. No fossettes are evident in the DP3 of UATF-V-002013 (Fig. 6A), but a conspicuous oval fossette is present near the midpoint of the distal border of this tooth in MNHN-BOL-V-003672 (Fig. 6E). It is formed by the distal cingulum joining the distal portions of the ectoloph and metaloph and is closed on the right side and nearly closed on the left. A similar fossette is present in DP2–3 of *Parastrapotherium* (Fig. 6B). A tiny fossette is present between the ectoloph and the crista in MNHN-BOL-V-003672. It is located closer to the distal branch of the central valley than the mesial one and could represent a buccal vestige of this structure or a vestige of the distal fossette. It is slightly larger on the left than on the right. In *X. kraglievichi*, the distal branch of the central valley is proportionately longer than in the QHB astrapothere, the mesial branch is curved rather than straight, and the crista separating these branches is comparatively long and narrow. The distal branch is more perpendicular to the lingual face of DP3 in *X. kraglievichi* than in the QH astrapothere. The occlusal surface of DP3 is complex in *Parastrapotherium* (see also Scott 1937), consisting of two well-defined fossettes that may represent remnants of the mesial and distal branches of the central valley. The central valley is sigmoid, directed first distally then mesially. The morphology of the more distal portion cannot be discerned with confidence due to poor preservation but may preserve a posterior fossette or flexus partially enclosed by a distal extension of the ectoloph. A cingulum is present along the mesial and lingual faces of DP3 in UATF-V-002013 that deepens to form an anterolingual pocket (Fig. 6A). A similar but shallower morphology (primarily due to wear) is present in MNHN-BOL-V-003672 and *X. kraglievichi* (Fig. 6D, E). No anterolingual pocket is present in *Parastrapotherium* sp., and the lingual cingulum is less pronounced (Fig. 6B).

The DP4s of MNHN-BOL-V-003672 are not fully erupted; the mesial and buccal portions of the occlusal surfaces of these teeth are slightly worn, but the distal portions are not, and neither is the most distal portion of protoloph (Figs. 5D, 6E). The parastyle and paracone folds together form a quadrangular buccomesial extension of the occlusal extension of the crown, and a narrow crista is present that extends lingually perpendicular to the ectoloph. A thin crest that could represent the crochet is connected to the distal side of the crista; it extends distally to define a depression in the occlusal surface that would likely form a fossette with additional wear (Fig. 6E). The more mesial depression, between the protoloph and the crista, represents the mesial branch of the central valley. A conspicuous cingulum is present along the mesial and lingual faces of the tooth. The DP4s of *Astrapotherium*? *ruderarium* Ameghino, 1902

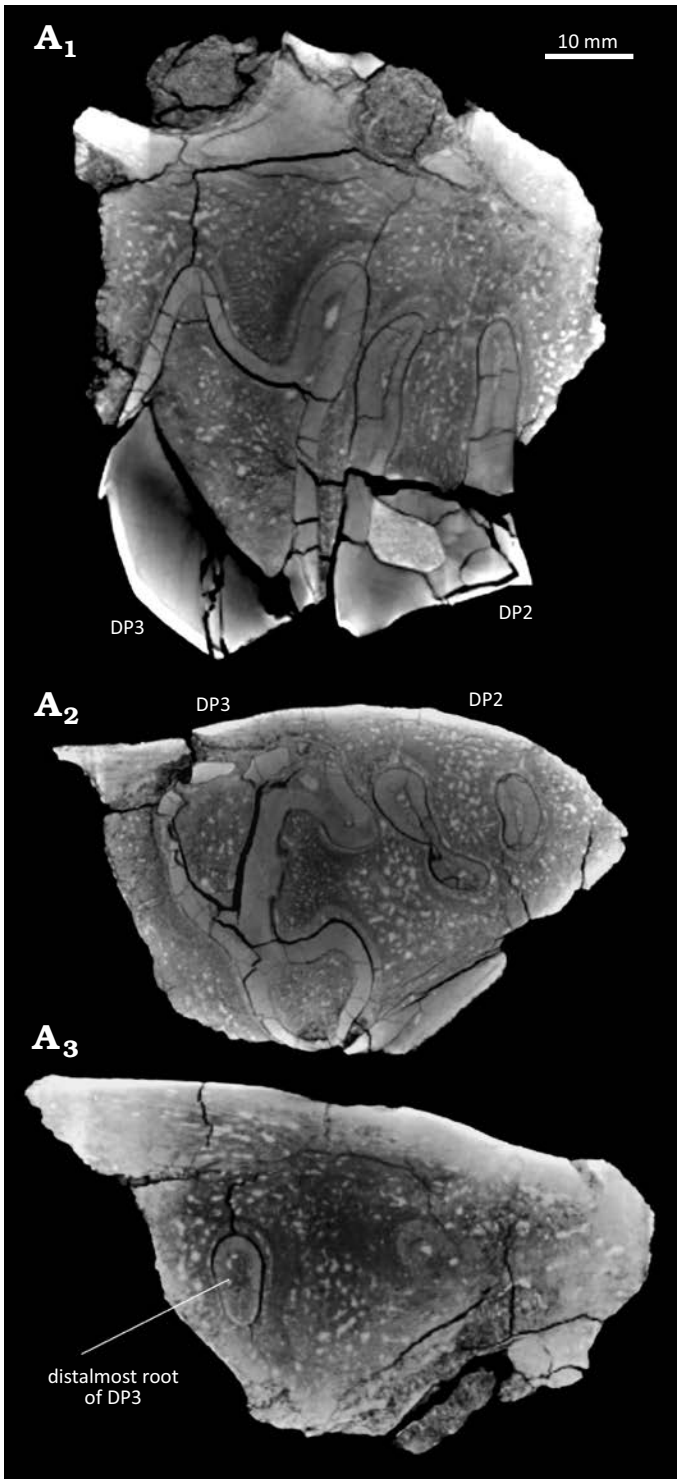

Fig. 8. Selected CT scan images of UATF-V-002013, Uruguaytheriinae gen.? et sp. nov. (upper Middle Miocene, QHB, Bolivia). Anterior is to the right in all images. A_1, Parasagittal slice, showing the two buccal roots of DP3 (left) and DP2 (right). A_2, Axial slice, showing the three roots of DP3 (left) and DP2 (right). A_3, Axial slice showing no signs of permanent teeth; note distalmost root of DP3 for reference.

(FMNH 13429) are heavily worn and preserve no cingulae or occlusal features such as fossettes or flexus. The greater wear accounts for their distinct proportions (i.e., greater breadth than length) relative to homologous teeth of other astrapotheres (Fig. 7; SOM 2). By contrast, the DP4 of *Xenastrapotherium chaparralensis* is completely unworn but only partially preserved (Stirton 1947: pl. 86: fig. 21). It is broadly similar to that of the QHB astrapothere, but it is not possible to distinguish differences of potential taxonomic value from those due to preservation and wear. A tooth that may represent DP4 of *Astrapotherium burmeisteri* (MACN-A 3300; Kramarz et al. 2019: supp data S1: fig. 2) has a more transversely oriented metaloph and distal cingulum; as a result, the tooth is much broader distally than in the QHB astrapothere, and the long axis of the posterior fossette is oriented at an angle relative to the toothrow rather than parallel to it. Other possible differences cannot be discerned with confidence due to their different wear states.

A CT scan of UATF-V-002013 shows no indication of permanent teeth above the deciduous premolars (Fig. $8A_1$, A_3). Both DP2 and DP3 have three roots (Fig. $8A_2$). The DP2 has two conjoined distal roots and a separate anterior root. The roots are oval in section, about twice as long buccolingually as mesiodistally. The roots curve lingually and decrease in size toward their tips. The buccal distal root is larger than the lingual root and is teardrop shaped in section, with the pointed edge on the lingual side; the lingual root is suboval in section. The mesial root is slightly larger than the lingual root, oval in section, and positioned near the buccolingual midpoint of the jaw. The mesial root is slightly closer to the lingual root than the buccal root. The pulp cavities of the roots increase in size further into the maxilla and mirror the shapes of the roots.

The DP3 roots are much larger than the DP2 roots (Fig. $8A_2$). Two buccal and one lingual root are present, all joined. The lingual root is more circular in section and about twice as large in both dimensions as each DP2 root. The buccal distal root is triangular in section, tapering lingually and slightly smaller than the lingual buccal root. The mesial root is the smallest of the three and oval in section. It is about three times as long buccolingually as mesiodistally. It is positioned closer to the buccal wall of the maxilla than the buccal DP2 roots. The DP3 roots curve lingually and decrease significantly in size toward their tips.

UATF-V-002013 preserves a partial lower incisor of uncertain position (Fig. 9A). We interpret it as a deciduous incisor based on its small size; it measures 13.4 × 6.9 mm at the base of the crown (mesiodistal × labiolingual diameter), about 60% the size of relatively unworn permanent lower incisors of *A. magnum* (mesiodistal diameter: 22–23 mm; Scott 1928: 339). However, it is comparable in size to a deciduous lower incisor preserved in YPM VPPU 15332 that measures ~14 mm mesiodistal diameter (based on available photographs). The incisor of UATF-V-002013 measures 47.5 mm from the occlusal surface to the root apex. It originally was bilobed, but only one of the lobes is preserved. The base of the broken lobe suggests that the two lobes were subequal in size. The tip of the preserved lobe is smoothly rounded and exhibits only a small amount of apical wear. A shallow sulcus separates the two lobes on both the labial and lingual faces,

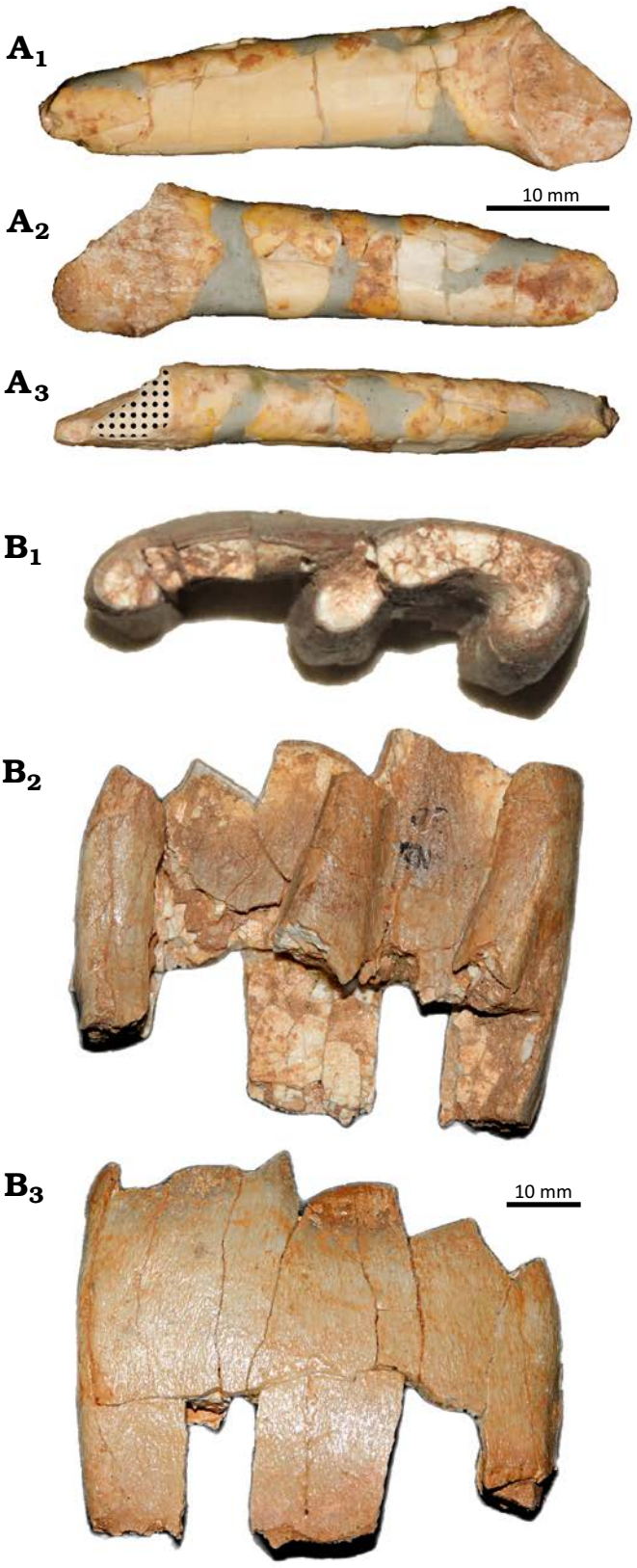

Fig. 9. Lower teeth referred to Uruguaytheriinae gen.? et sp. nov. from the Quebrada Honda Basin, Bolivia (upper Middle Miocene). **A**. UATF-V-002013, deciduous lower incisor, in lingual (A_1), labial (A_2), and mesial or distal (A_3) views. **B**. MNHN.F.BLV 46, m3, in occlusal (B_1), lingual (B_2), and buccal (B_3) views.

but the latter is more pronounced. The cingulid is closely appressed to the labial side of the tooth and bears crenate lobes that extend toward the occlusal surface. On the lingual face, the cingulid is a well-developed shelf. It is straight near the middle of the lingual face and curves upwards toward the mesial and distal sides, forming a slightly greater angle relative to horizontal on the broken side of the tooth.

MNHN.F.BLV 46 includes many tooth and bone pieces, most of which are too fragmentary to be described. The most complete tooth is a left m3, composed of many pieces that were glued together (Fig. 9B). Other identifiable pieces include most of a right m3 (including the occlusal surface) and fragments of both M3s (SOM 4). All molar fragments are little worn, and only the anterior ectoloph fragment of the right M3 has a visible wear facet. In both m3s, only small portions of the occlusal enamel are preserved: the mesial face of the paralophid and the mesialmost portion of the external surface of the talonid. The paralophid, metalophid, and hypolophid are distinct from one another and separated by the paraflexid and entoflexid. The only suggestion of a hypoflexid is a subtle concavity near the occlusal surface of the tooth that is only visible in occlusal view. The paraflexid is slightly deeper (i.e., more penetrating) than the entoflexid. Both appear quite deep due to the relatively unworn state of the tooth (cf. Kramarz et al. 2019). The entoflexid is oriented obliquely as in other uruguaytheriines except *U. beaulieui*. The lophids are rounded, anteroposteriorly narrow, and widen towards the base. The paralophid creates an almost flat anterior wall, curving slightly posteriorly. There is no sign of a "pillar" attached to the metaconid. The anterior ectoloph fragment of the right M3 shows a well-developed paracone fold and conspicuous parastyle. The lingual fragment of right M3 preserves a narrow protoloph with a well-developed lingual cingulum. There is no connection between the protoloph and metaloph of the M3 (i.e., the central valley is open lingually), unlike the condition in *X. kraglievichi, X. amazonense*, and *X. chaparralensis* (Johnson and Madden 1997), as well as *H. castanedaii* (Vallejo-Pareja et al. 2015). The anterolingual pocket is not visible in occlusal view but deepens closer to the base of the crown as has been noted for other uruguaytheriines such as *G. snorki* (Croft et al. 2020a).

UF 563068 includes four tooth and enamel fragments, three of which are shown in SOM 5. One of these fragments is the distolingual portion of a left upper molar that preserves the floor of the median fossette and the posterior branch of the lingual flexus. Other fragments include a large piece of enamel (ca. 55 mm × 14 mm), likely from of an upper molar ectoloph, and a small piece of enamel and dentin from an occlusal surface that preserves part of the labial fold of the paracone. None of these remains is diagnostic beyond the family level.

Remarks.—Although fragmentary, astrapothere remains from the QHB do not compare closely with any recognized species. This is reflected in its intermediate size as well as discrete morphological features of the deciduous and

permanent dentition, including much greater hypsodonty. Considering these differences, we refrain from referring the new species to any currently recognized genus.

Hoffstetter (1977) listed 7 cm as the length of both M3 and m3 of MNHN.F.BLV 46, implying that the specimen preserves a complete (or reasonably complete) M3. This may have been the case when the specimen was collected, but at present, MNHN.F.BLV 46 only includes tooth fragments (and bone fragments) besides the left m3 described above. Some M3 fragments include useful morphological information, but they do not form a significant portion of a M3 that can be measured. According to our measurements, the length of the left m3 is 66.8 mm, the width is 20.6 mm, and the maximum crown height is 55.2 mm.

UF 26679 includes two toxodontid notoungulate left lower molars (an m3 and a likely m1) in addition to astrapothere tooth and bone fragments. Two notes associated with UF 26679 indicate that enamel samples for $\delta^{13}C$ analysis were taken from both a toxodontid tooth and an astrapothere tooth of this specimen. The results of these analyses were published by MacFadden et al. (1994) and are discussed below.

Mesowear angle results

The lower molar facet angles measured in UATF-V- 001052, UATF-V-001054 and UATF-V-001981 are high (>160°) (Table 1), indicating a diet very low in abrasion. The mean lower molar facet angle of 163.8° is consistent with those measured in browsing rhinos (e.g., *Diceros bicornis*) by Hernesniemi et al. (2011), although these authors found substantial variation within modern rhino species samples. The three MAs measured from upper cheek teeth (UATF-V-002013, UF 26679, and MNHN.F.BLV 46) are also sharp (81°, 84°, and 84°, respectively), similar to upper tooth values from modern browsing rhinos (Wilson and Saarinen 2024b).

Table 1. Mesowear angles measured from Middle Miocene Bolivian astrapothere specimens. Lower molar angles were measured from the wear facet to the buccal surface of the tooth (Hernesniemi et al. 2011). For upper molars, facet inclination (FI) was converted to a mesowear angle (MA) using the equation MA = 180° – (2 × FI). The facet inclination was measured as the angle of the wear facet of the ectoloph relative to the rest of the occlusal surface of the tooth.

Specimen	Locality	Molar	Mesowear angle
UATF-V-001052	Nazareno	lower	162.5°
UATF-V-001054	Nazareno	lower	163°
UATF-V-001981	Cerdas	lower	166°
MNHN.F.BOL 46	Quebrada Honda	upper	84°
UATF-V-002013	Quebrada Honda	upper	81°
UF 26679	Quebrada Honda	upper	84°

Isotope results

Mean and range $\delta^{13}C$ values for the species (N = 3) and specimens (N = 16) analyzed are presented in Table 2; data for each sample analyzed (N = 92) are presented in SOM 6. Species means for proterotheriid litopterns (*Olisanophus* spp.) and the hegetotheriid notoungulate *H. trilobus* are indistinguishable from one another (both are 10.6‰) and 1.1‰

Table 2. Summary $\delta^{13}C$ values (‰, relative to the Vienna PeeDee Belemnite) for each UATF specimen analyzed, including number of samples per specimen (#), mean value for all samples, minimum and maximum values (Min. and Max., respectively), and range between lowest and highest values. Values for each sample are listed in SOM 6. Specimens are grouped by species and include a species or genus mean for each summary statistic. Local areas and geological sub-units of the QHB follow Gibert et al. (2020) and Saylor et al. (2022).

Specimen	Taxon	Local area	Sub-unit	#	Mean	Min.	Max.	Range
UATF-V-000951	*Olisanophus* sp. indet.	Quebrada Honda	A-lower	2	-10.5	-10.6	-10.4	0.2
UATF-V-000978	*Olisanophus akilachuta*	Rio Rosario	A-lower	5	-10.3	-11.9	-9.6	2.3
UATF-V-001287	*Olisanophus riorosarioensis*	Rio Rosario	A-lower	5	-10.0	-10.3	-9.6	0.7
UATF-V-001780	*Olisanophus akilachuta*	Quebrada Honda	A-middle	3	-11.7	-11.9	-11.4	0.5
Mean					-10.6	-11.2	-10.3	0.9
UATF-V-000890	*Hemihegetotherium trilobus*	Quebrada Honda	A-lower	6	-11.8	-12.4	-11.4	1.0
UATF-V-000986	*Hemihegetotherium trilobus*	Rio Rosario	A-lower	3	-10.5	-10.9	-10.2	0.7
UATF-V-001131	*Hemihegetotherium trilobus*	Huayllajara	A-upper	5	-10.2	-10.3	-10.0	0.3
UATF-V-001209	*Hemihegetotherium trilobus*	Huayllajara	B-upper	6	-10.5	-11.6	-9.9	1.7
UATF-V-001236	*Hemihegetotherium trilobus*	Huayllajara	B-upper	3	-10.0	-10.1	-9.9	0.2
Mean					-10.6	-11.1	-10.3	0.8
UATF-V-001028	Toxodontidae sp. indet.	Rio Rosario	A-lower	8	-9.8	-10.9	-9.1	1.8
UATF-V-001290	Toxodontidae sp. indet.	Rio Rosario	A-lower	8	-9.6	-10.6	-9.1	1.5
UATF-V-001528	Toxodontidae sp. indet.	Rio Rosario	A-lower	8	-9.3	-10.6	-8.7	1.9
UATF-V-001588	Toxodontidae sp. indet.	Rio Rosario	A-lower	8	-9.4	-10.0	-9.0	1.0
UATF-V-001769	Toxodontidae sp. indet.	Quebrada Honda	A-lower	8	-9.3	-9.6	-9.0	0.6
UATF-V-001933	Toxodontidae sp. indet.	Quebrada Honda	A-middle	8	-9.6	-9.8	-9.4	0.4
UATF-V-001956	Toxodontidae sp. indet.	Quebrada Honda	A-middle	6	-9.3	-11.0	-7.6	3.4
Mean					-9.5	-10.4	-8.8	1.5

Table 3. Published enamel carbon isotope data ($\delta^{13}C$, ‰, relative to the Vienna PeeDee Belemnite) from Bolivian late Oligocene and Miocene notoungulates, astrapotheres, and pyrotheres and Argentine astrapotheres. Revised $\delta^{13}C$ values were recalculated using body-mass-specific enrichment factors (see text and SOM 1 for details, including updated taxonomic identifications). Sources: B10, Bershaw et al. (2010); M94, MacFadden et al. (1994); M96, MacFadden et al. (1996). Localities are listed in reverse chronological order (by Ma, megannum), and ages for localities other than the QHB are based on MacFadden et al. (1990, 1995; Micaña, Quehua, Cerdas), Fernández-Monescillo et al. (2019; Achiri), Perkins et al. (2012; Santa Cruz and Pinturas formations), and Kay et al. (1998; Salla). Asterisks denote values indicative of possible C4 grazing (*; −8.2‰ to −7.0‰) and unequivocal C4 grazing (**; > -7.0‰) from Ward et al. (2024).

Sample No.	Source	Taxon	Locality	$\delta^{13}C$	$\delta^{13}C$ Revised
56	M94	*Microtypotherium choquecotense*	Micaña, Bolivia (~7.5 Ma)	-7.0	-7.6*
31	M94	*Plesiotypotherium* sp.	Quehua, Bolivia (~10–9 Ma)	-7.7	-7.9*
34	M94	*Plesiotypotherium* sp.	Quehua, Bolivia (~10–9 Ma)	-5.5	-5.7**
54	M94	*Plesiotypotherium* sp.	Quehua, Bolivia (~10–9 Ma)	-5.9	-6.1**
20	M94	*Plesiotypotherium achirense*	Achiri, Bolivia (~10.5–9.5 Ma)	-8.2	-8.4
(mean ± s.d.)	B10	Toxodontidae indet.	Achiri, Bolivia (~10.5–9.5 Ma)	-8.7 ± 0.6	-8.9 ± 0.6
52	M94	*Hemihegetotherium trilobus*	QHB, Bolivia (~13–12 Ma)	-9.7	-10.4
27	M94	Toxodontidae sp. indet.	QHB, Bolivia (~13–12 Ma)	-10.4	-9.6
50	M94	Toxodontidae sp. indet.	QHB, Bolivia (~13–12 Ma)	-9.5	-8.7
51	M94	Toxodontidae sp. indet.	QHB, Bolivia (~13–12 Ma)	-10.5	-9.7
28 (UF 26679)	M94	Uruguaytheriinae gen. et sp. nov.	QHB, Bolivia (~13–12 Ma)	-10.7	-9.7
37	M94	*Palyeidodon* sp.	Cerdas, Bolivia (~16–15 Ma)	-7.9	-7.1*
53	M94	*Palyeidodon* sp.	Cerdas, Bolivia (~16–15 Ma)	-7.5	-6.7**
95-56/C2184	M96	*Astrapotherium magnum*	Santa Cruz Fm., Argentina (~18–16 Ma)	-11.8	-10.8
SC-7/C1292	M96	*Astrapothericulus iheringi*	Pinturas Fm., Argentina (~18–17 Ma)	-9.8	-9.2
SC-8/C1293	M96	*Astrapothericulus iheringi*	Pinturas Fm., Argentina (~18–17 Ma)	-12.1	-11.5
SC-9/C1297	M96	*Astrapothericulus iheringi*	Pinturas Fm., Argentina (~18–17 Ma)	-10.2	-9.6
23	M94	*Anayatherium* sp.	Salla, Bolivia (~29–25 Ma)	-10.3	-9.7
(mean ± s.d.)	B10	*Eurygenium pacegnum*	Salla, Bolivia (~29–25 Ma)	-10.4 ± 0.5	-11.5 ± 0.5
16	M94	*Rhynchippus* cf. *R. brasiliensis*	Salla, Bolivia (~29–25 Ma)	-9.5	-9.6
17	M94	*Rhynchippus* cf. *R. brasiliensis*	Salla, Bolivia (~29–25 Ma)	-10.7	-10.8
33	M94	*Rhynchippus* cf. *R. brasiliensis*	Salla, Bolivia (~29–25 Ma)	-9.1	-9.2
22	M94	*Trachytherus alloxus*	Salla, Bolivia (~29–25 Ma)	-9.6	-10
(mean ± s.d.)	B10	*Trachytherus alloxus*	Salla, Bolivia (~29–25 Ma)	-9.0 ± 0.4	-10.4 ± 0.4
(mean ± s.d.)	B10	*Pyrotherium macfaddeni*	Salla, Bolivia (~29–25 Ma)	-7.8 ± 0.4	-7.9 ± 0.4
19A	M94	*Pyrotherium* sp.	Salla, Bolivia (~29-25 Ma)	-9.2	-8.3
24	M94	*Pyrotherium* sp.	Salla, Bolivia (~29–25 Ma)	-8.7	-7.6*
32	M94	*Pyrotherium* sp.	Salla, Bolivia (~29–25 Ma)	-8.4	-7.4*

lower than the corresponding mean for the toxodontid notoungulate (Table 2). A similar pattern applies to minimum and maximum $\delta^{13}C$ values for each specimen, which span -11.9‰ to -9.6‰ for *Olisanophus* spp., -12.4‰ to -9.9‰ for *H. trilobus*, and -11.0‰ to -7.6‰ for the toxodontid. Overall, toxodontid specimens vary most in $\delta^{13}C$ values; the mean range per specimen (1.5‰) is more than 50% greater than that of *Olisanophus* spp. and *H. trilobus* (0.9‰ and 0.8‰, respectively). Additionally, one toxodontid has the greatest range of any QHB specimen (3.4‰). It is an outlier even compared to other toxodontid specimens; its three most positive samples are beyond the range of samples from remaining toxodontid specimens (-8.6‰, -7.8‰, and -7.6‰). Specimens of *Olisanophus* spp. are generally the least variable among QHB specimens (0.2–0.7‰). However, one specimen of *O. akilachuta* has a range of 2.3‰, more than triple that of any other *Olisanophus* specimen. Unlike the highly variable toxodontid specimen, neither the minimum nor maximum sample value is beyond the range of other *Olisanophus* specimens.

Regarding local areas within the QHB, specimens of *Olisanophus* spp. and *H. trilobus* from the Quebrada Honda Local Area have more negative mean $\delta^{13}C$ values and tend to have more negative ranges than those from the Río Rosario and Huayllajara local areas, though there is some overlap in values (Table 2). This pattern does not hold for the toxodontid. Similarly, there is no clear correlation between $\delta^{13}C$ values and stratigraphic sub-unit in any taxon.

Our new herbivore $\delta^{13}C$ values from the QHB are highly congruent with those published by MacFadden et al. (1994) when diet-bioapatite (enamel) enrichment factors (ε^*) are used; their single *H. trilobus* value and their three toxodontid values are close to our new mean values for these notoungulates (Tables 2, 3). Their value for the QHB astrapothere (-9.7‰) is just below our species mean for the QHB toxodontid (-9.5‰). This value falls within the

relatively broad range (2.3‰) of values of Early Miocene astrapotheres analyzed by MacFadden et al. (1996) but is closer to the higher end of the bimodal distribution (Table 3; see also below).

Discussion

The limited astrapothere remains currently known from the QHB do not permit a precise taxonomic identification. Nevertheless, the evidence at hand suggests that they do not pertain to any currently recognized species or even genus. If correct, this conclusion reinforces a pattern seen in other QHB mammals; more than 80% of formally described QHB species have not been recorded elsewhere, and no QHB species has been unequivocally recorded at La Venta (Strömberg et al. 2024). At higher taxonomic levels (genera, subfamilies, and families), the QHB fauna is more similar to those of southern South America than low-latitude ones such as La Venta (Croft 2007; Croft et al. 2011; Strömberg et al. 2024). Interestingly, astrapotheres are an exception to this pattern; during the late Middle Miocene, Astrapotheriidae (Astrapotheria) is the only suprageneric mammal clade present at middle- and low-latitude sites (including the QHB and La Venta) but not high-latitude ones. All other groups of terrestrial mammals shared by the QHB and La Venta had essentially continent-wide distributions during the late Middle Miocene (e.g., interatheriid and toxodontid notoungulates, macraucheniid litopterns, megatheriid sloths, etc.; Strömberg et al. 2024: fig. 8). This atypical distribution is likely related to the paleoenvironmental requirements of astrapotheres; suitable areas had apparently disappeared from the southern third of the continent by the late Middle Miocene, coincident with the Middle Miocene Climatic Transition (Croft et al. 2016). The extinction of astrapotheres by the end of the Middle Miocene suggests that further climatic deterioration eliminated the suitable habitat that remained at lower latitudes as well.

Mesowear angles and astrapothere diets.—Although the number of specimens available for mesowear angle (MA) analysis is relatively low, in combination, our results suggest that Bolivian astrapotheres were consuming a low-abrasion diet consistent with browsing. The sharp lower molar facet angles are analogous to those of modern browsing rhinos (*Diceros bicornis*, *Dicerorhinus sumatrensis*, and *Rhinoceros sondaicus*) (Hernesniemi et al. 2011), and the MAs of UATF-V-002013 (81°), MNHN.F.BLV 46 (84°), and UF 26679 (84°) are similar to those observed in the upper teeth of these species (Wilson and Saarinen 2024b). Very sharp mesowear angles (< 90°) could be the result of attritional wear produced by consuming of particularly tough foods like twigs and branches, which would be expected to sharpen facets (Popowics and Fortelius 1997). Our results suggest that such material might have formed a major component of the diets of Middle Miocene Bolivian astrapotheres. This inference is consistent with the suggestion that vertical enamel prism decussation in astrapotheres, which is evident in specimens from the QHB, Nazareno and Cerdas, is an adaptation for consuming foods that produce high mechanical stresses (Rensberger and Pfretzschner 1992; Rensberger 2004).

Our Bolivian astrapothere mesowear results are also concordant with previously reported paleoenvironmental reconstructions for these localities. For example, the environment of the QHB has been reconstructed as being similar to a modern semi-deciduous/dry forest and/or wooded savanna (Catena et al. 2017; Catena and Croft 2020; Strömberg et al. 2024), where abundant browse in the form of both trees and shrubs would have been available for astrapotheres. By extension, these large ungulates may have occupied an ecological niche analogous to extant black rhinos (*Diceros bicornis*) in African savannas. Paleoenvironmental reconstructions of Cerdas suggest that it was more open and less productive than the QHB, likely representing a variably open shrubland (Croft et al. 2009, 2016; Catena et al. 2016). A similar environment may have been present at Nazareno, considering the similarities between its fauna and that of Cerdas (Croft and Anaya 2020). Our MA results suggest that astrapotheres at both Nazareno and Cerdas were consuming woody materials, implying that sufficient shrubby browse must have been available to sustain a population of very large herbivores. Future paleoenvironmental studies at these sites may be able to test this hypothesis.

In general, Miocene astrapotheres have been interpreted as browsers based on their relatively low-crowned teeth (e.g., Simpson 1980; Johnson and Madden 1997; Croft 2016), an inference compatible with our MA angle data and dietary interpretations. By contrast, Cassini et al. (2012) reconstructed late Early Miocene *Astrapotherium* (from the Santa Cruz Formation, Argentina) as a mixed feeder using linear measurements of the skull and a comparative dataset of extant artiodactyls and perissodactyls from Mendoza et al. (2002). Regarding *Astrapotherium*, Scott (1937: 534) noted that "All parts of this skeleton are peculiar and exceptional, but the skull and feet are the most remarkable of all and, outside of the family, no known mammal has a skull in the least like it, save, of course, such features as are common to all hoofed mammals whatsoever." We agree with Scott's (1937) characterization. Although it is possible that *Astrapotherium* from the Santa Cruz Formation had a diet very different than those of Bolivian astrapotheres, it is also possible that the cranial anatomy of *Astrapotherium* is too distinctive to result in reliable dietary interpretations when comparisons are solely based on extant ungulates.

The relatively hypsodont deciduous dentition of the QHB astrapothere is noteworthy and suggests that the species may have had different habitat preferences from other astrapotheres despite a similar browsing diet. We acknowledge that studies of hypsodonty (in general) have focused on the permanent rather than the deciduous dentition, but extant rhinos may represent an analogous situation if the

permanent dentition of the QHB astrapothere is similarly more hypsodont than other taxa. For example, Wilson and Saarinen (2024b) found broadly similar mesowear angles in black rhinos (*Diceros bicornis*) and Sumatran rhinos (*Dicerorhinus sumatrensis*; 77.3° and 75°, respectively) even though these species differ markedly in their hypsodonty indices (2.24 and 1.67, respectively; Janis 1988). Although both species are browsers, the more hypsodont black rhino does not inhabit humid rainforests (Ritchie 1963; Rookmaaker and Antoine 2012); instead, it prefers more open habitats (Goddard 1970; Loutit et al. 1987; Kotze and Zacharias 1993; Buk and Knight 2010), which are characterized by higher levels of exogenous abrasives on plants (e.g., dirt and dust). Hypsodonty in the black rhino and other mammals represents an adaptation to counteract increased tooth wear resulting from higher levels of exogenous abrasives and is correlated with both habitat and diet (Janis and Fortelius 1988; Damuth and Janis 2011). Since mesowear reflects only diet in extant mammals (Kaiser et al. 2013), systematic analyses of both hypsodonty and mesowear in astrapotheres from diverse localities might reveal patterns that allow them to be used as paleoenvironmental indicators, as has been suggested for some other groups of South American native ungulates (Patterson and Pascual 1968, McGrath et al. 2020; Wilson and Saarinen 2024a). The greater hypsodonty of the QHB astrapothere compared to contemporaneous species such as *X. kraglievichi* could reflect the more open habitat of QHB relative to La Venta, as has been reconstructed based on other types of evidence (Strömberg et al. 2024).

Stable carbon isotopes.—Stable carbon isotope ($\delta^{13}C$) data suggest that astrapotheres and toxodontids in the QHB consumed plants of similar isotopic composition (Table 2). As noted above, the single value for the QHB astrapothere (-9.7‰) is very close to the mean for QHB toxodontids (-9.5‰) and well within the toxodontid range. The QHB astrapothere value is nearly 1‰ more positive than mean values for *Olisanophus* spp. and *H. trilobus* and nearly outside the range of specimens of both (two *Olisanophus* spp. have maximum values of -9.6‰). This suggests dietary niche partitioning between the astrapothere and these smaller herbivores. Sampling additional astrapothere specimens is necessary to assess if these patterns are real or due to small sample size.

None of the QHB species analyzed has values typical of closed habitat browsers (≤ -12.5‰; Ward et al. 2024). This is congruent with paleoenvironmental interpretations for the QHB noted above, none of which suggests the area was covered by closed-canopy forest in the late Middle Miocene. Carbon isotope values from nearly all QHB herbivore samples are within the range expected for herbivores feeding in open-canopy habitats (-12.5‰ to -8.2‰). The sole exceptions are two samples of -7.8‰ and 7.6‰ from toxodontid specimen UATF-V-001956 (SOM 6), which fall within the range of grazers feeding on water-stressed C3 vegetation or small amounts (≤ 20%) of C4 grasses (Ward et al. 2024). Either scenario is plausible based on current interpretations of the QHB paleoenvironment. Since C4 grasses are thought to have comprised only a small proportion of subtropical South American vegetation prior to their Late Miocene expansion ca. 9 million years ago (Hynek et al. 2012), an interval of aridity may be the more likely explanation. However, $\delta^{13}C$ data from the toxodontid *Palyeidodon* sp. from the slightly older site of Cerdas suggest that feeding on C4 grasses should not be ruled out as a possible explanation for positive $\delta^{13}C$ values in the QHB; although only two samples were analyzed, one is within the range of unequivocal C4 grazers, and the other is only slightly more negative (Table 3; this is discussed further below).

Few other $\delta^{13}C$ data are available for astrapotheres. MacFadden et al. (1996) published $\delta^{13}C$ data for four specimens from the upper Lower Miocene (Burdigalian) of Santa Cruz Province, Argentina. Recalculated values for these specimens are roughly bimodal within the range of C3 browsers in open-canopy habitats (Table 3); two specimens are near the upper end of the range, with values similar to the QHB astrapothere (-9.6‰ and -9.2‰), whereas two others are closer to the lower end of the range (-11.5‰ and -10.8‰). This range of values (2.3‰) is similar to that seen in QHB toxodontids, suggesting that the QHB astrapothere may have consumed plants with a similarly broad range of $\delta^{13}C$ values. The single value from *Astrapotherium magnum* from the Santa Cruz Formation is within the range of values from *Astrapothericulus iheringi* from the Pinturas Formation (Table 3), implying no major dietary differences between these species despite possible differences in habitats represented by these formations (see McGrath et al. 2023 for a recent discussion).

Hoerner (2017) provided $\delta^{13}C$ data from four indeterminate La Venta astrapothere specimens in her dissertation. Bulk values for these specimens range from -12.35 to -11.39 (mean = -11.74), and serial sample values from two specimens range from -12.63 to -10.94, broadly similar to those obtained for Argentine and Bolivian astrapotheres. These slightly more negative values could reflect denser vegetation at La Venta (Kay and Madden 1997; Catena and Croft 2020) or differences in apparent diet-bioapatite enrichment factors; Hoerner (2017) did not explicitly mention the enrichment value she used, so we were unable to recalculate them to ensure direct comparability to ours and those of MacFadden et al. (1994, 1996).

Miocene paleoenvironments and paleoelevations in Bolivia.—Several types of evidence indicate that the QHB had a seasonal, tropical to subtropical climate (i.e., mean annual temperature > ~20°C) with moderate precipitation (800–1400 mm/year) during the late Middle Miocene, resulting in a mosaic landscape akin to a modern dry forest or wooded savanna with no close modern analog (Cadena et al. 2015; Catena et al. 2017; Catena and Croft 2020; Gibert et al. 2020; Saylor et al. 2022; Strömberg et al. 2024). Our inferences about astrapothere paleoecology are consistent

with this paleoenvironmental reconstruction. By contrast, paleotemperature estimates based on clumped isotope paleothermometry suggest a much lower mean annual air temperature (MAAT) of 9 ± 5°C for the QHB (Garzione et al. 2014). This discrepancy could reflect problems with isotopic sampling in the QHB (e.g., sampling at greater depth in the paleosol would result in erroneously low inferred MAAT; Catena et al. 2017). The presence of apparent outliers among the seven QHB samples analyzed raises additional questions about these estimates; most values (5/7) yield reconstructed MAATs of 10–15°, but two are beyond the range of credible paleotemperatures for the QHB based on floral and faunal data (2 and 7°C; Garzione et al. 2014: table 1).

Garzione et al. (2014) also used clumped isotope paleothermometry to estimate MAAT at Cerdas (mentioned previously) and Quehua, a Late Miocene site located ca. 115 km to the northwest (see also MacFadden et al. 1995). Their results suggest MAAT about 10°C warmer at Cerdas than at the QHB (19 ± 9°C) and about 7°C colder at Quehua (2 ± 4°C), only slightly colder than estimates for a modern soil at Quehua analyzed using the same method (0 ± 7°C). Based on these inferred temperatures, Garzione et al. (2014) concluded that the southern Altiplano experienced ~1.5 km of uplift between the time of Cerdas and the QHB and an additional ~1 km of uplift prior to the time of Quehua, resulting in essentially modern paleoelevations in the southern Central Andean Plateau by the Late Miocene (Garzione et al. 2017).

The presence of environmentally sensitive astrapotheres at both Cerdas and the QHB (as well as at Nazareno) argues against any significant decrease in MAAT during the Middle Miocene as inferred by Garzione et al. (2014, 2017). Our paleontological data suggest that Cerdas-like temperatures predominated in southern Bolivia at least throughout the Middle Miocene. This, in turn, implies that the region did not experience significant uplift during this interval.

Although $\delta^{13}C$ data from fossilized herbivore teeth cannot be used to infer MAAT (or paleoelevation) directly, they can provide indirect paleotemperature information because warmer growing season temperatures (and lower atmospheric CO_2) favor C4 grasses relative to C3 grasses (Teeri and Stowe 1976; Edwards et al. 2010; Hynek et al. 2012). Since temperature decreases with elevation, the proportion of C4 grasses also decreases with elevation (Edwards et al. 2010; de Deus Vidal et al. 2021 and references therein). In modern grass-dominated mountain systems, the point at which C3 grasses become taxonomically dominant over C4 grasses has been termed the "grass-line" (de Deus Vidal et al. 2021). Globally, this transition occurs around 14.6°C mean annual temperature; in South America, it occurs at 20.2°C in Colombia (4°N) and 13.0°C in Argentina (32°S) (de Deus Vidal et al. 2021).

Hynek et al. (2012) suggested that late Neogene fossil sites in Bolivia were likely too high for C4 plants to flourish. Nonetheless, MacFadden et al. (1994) noted that $\delta^{13}C$ values from the Bolivian Miocene sites of Cerdas, Achiri, and Micaña are too high to be attributable exclusively to C3 vegetation, likely indicating the presence of temperate and tropical C4 grasses. Indeed, two of the three values from Quehua unequivocally indicate C4 grazing (Table 3). It is difficult to reconcile the presence of C4 grasses with the low paleotemperature and high paleoelevation inferred for Quehua by Garzione et al. (2014), particularly considering that slightly higher atmospheric CO_2 levels during the Late Miocene (The CenCO_2PIP Consortium 2023) would have resulted in a slightly lower grass-line. A possible explanation is that the herbivore enamel specimens from Quehua analyzed by MacFadden et al. (1994) were collected from a lower stratigraphic level than the carbonate samples analyzed by Garzione et al. (2014) and predate the inferred uplift. MacFadden et al. (1994) estimated the age of their samples at 10–9 Ma, which matches the age of the Quehua fossil horizon subsequently illustrated by MacFadden et al. (1995: fig. 7). Garzione et al. (2014) listed the ages of their samples as spanning 8.98–7.14 Ma, which suggests they were collected from slightly higher in the same section (Section 1, Chiu Chiu). This would leave a short interval between the two types of samples during which the uplift could have occurred. Although this scenario is possible, a more parsimonious explanation is that both Quehua and the QHB were at relatively low elevations during the Middle and Late Miocene (as has long been inferred based on paleobotanical evidence; Gregory-Wodzicki 2000, 2002; Garzione et al. 2008) and that uplift of the southern Bolivian Altiplano occurred concurrently with the northern Altiplano after ~9 Ma.

Conclusions

Only fragmentary astrapothere specimens have been collected from Middle Miocene sites in southern Bolivia, but they provide valuable insights into the diversity and distribution of this group during the final interval in which it is recorded in the fossil record. These remains also yield paleobiological data suitable for reconstructing Middle Miocene habitats in South America. The five astrapothere specimens from the late Middle Miocene Quebrada Honda Basin (QHB) represent a new species of uncertain generic affinities that remains unnamed pending recovery of more complete materials. The QHB species could represent a new genus, perhaps the same one present at the early Middle Miocene site of Cerdas, located ca. 170 km to the northeast. The QHB astrapothere is characterized by its intermediate size and relatively high-crowned deciduous dentition, among other features. Astrapothere specimens collected from the QHB thus far span the Quebrada Honda and Río Rosario local areas and strata ranging from the bottom of sub-unit A-lower to the lower part of sub-unit B-lower, a temporal interval of 300 000 to 900 000 years. Molar mesowear angle data and enamel-derived stable carbon isotope ($\delta^{13}C$) data from the QHB, Cerdas, and Nazareno (an early Middle Miocene site ca. 100 km

southeast of Cerdas) suggest that Early to Middle Miocene astrapotheres were browsers that may have had dietary habits similar to the extant black rhino (*Diceros bicornis*). We propose that Middle Miocene astrapotheres are likely reliable indicators of subtropical to tropical mean annual temperatures and that their extinction prior to the Late Miocene was primarily due to decreasing global temperatures and concomitant loss of suitable habitat. Enamel-derived stable carbon isotope data from Cerdas and Quehua (a Late Miocene site ca. 115 km to the northwest) suggest that some Middle and Late Miocene notoungulates were C4 grazers and that C4 grasses were relatively abundant in parts of southern Bolivia during this interval. The well-established positive relationship between the abundance of C4 grasses and warm growing season temperatures reinforces paleoclimatic interpretations for these and other sites based on other types of evidence and casts additional doubt on the conclusion that relatively cold temperatures (and high elevations) characterized the southern Central Andes prior to about 9 million years ago.

Acknowledgements

For access to specimens in their care, we thank: Ken Angielczyk and William Simpson (both Field Museum, Chicago, USA); Pat Holroyd (UC Museum of Paleontology, University of California, Berkeley, USA); Leopoldo González Oviedo (IGM); Bernardino Mamani Quispe (MNHN-BOL-V); Shirley Anahi Lugo Flores and Alejandra Morodías Ríos (both UATF) and Guillaume Billet and Christian de Muizon (both MNHN). We thank Beth Carroll, Amanda McGee, and Michael Ryan (all Cleveland Museum of Natural History, Cleveland, USA) for facilitating preparation of UATF-V-002013; Thure Cerling and Suvankar Chakraborty (both University of Utah, Salt Lake City, USA) for assistance with isotopic analyses of QHB samples; Bruce MacFadden and Rachel Narducci (both UF) and G. Billet for providing photographs and unpublished information about QHB specimens and samples; Alejandro Kramarz (Museo Argentino de Ciencas Naturales "Bernardino Rivadavia", Buenos Aires, Argentina) for providing photographs of YPM-VPPU 15332; Laura Chornogubsky (Museo Argentino de Ciencas Naturales "Bernardino Rivadavia", Buenos Aires, Argentina) for providing photographs and measurements of MACN-A 2399; and A. Kramarz and Beverly Saylor (Case Western Reserve University, Cleveland, USA) for helpful information and discussions that improved this contribution. The final manuscript was improved thanks to thorough and constructive reviews by A. Kramarz and an anonymous reviewer. We gratefully acknowledge the efforts of all members of the Bolivian and international field crews who collected the specimens at Cerdas, Nazareno, and the QHB that made this study possible. We specifically acknowledge Taryn Black (University of Washington, USA), who fortuitously discovered UATF-V-002013 while sampling for phytoliths. Funding for this research was provided by the National Science Foundation (EAR 0958733 and 1423058 to DAC) and the National Geographic Foundation (NGS 8115-06 to DAC). In addition, OW was supported by the Research Council of Finland (grant 340775/346292: NEPA/Non-Analogue Ecosystems of the Past), and the isotopic analyses were made possible by NSF 1137336: Inter-university Training in Continental-scale Ecology).

Editor: Eli Amson

References

Ameghino, F. 1887. Enumeración sistemática de las especies de mamíferos fósiles coleccionados por Carlos Ameghino en los terrenos eocenos de la Patagonia austral y depositados en el Museo La Plata. *Boletín del Museo de La Plata* 1: 1–26.

Ameghino, F. 1888. *Rápidas diagnosis de algunos mamíferos fósiles nuevos de la República Argentina*. 17 pp. Pablo E. Coni é hijos, Buenos Aires.

Ameghino, F. 1895. Premiere contribution à la connaissance de la faune mammalogique des couches à *Pyrotherium*. *Boletín del Instituto Geográfico Argentino* 15: 603–660.

Ameghino, F. 1899. *Sinopsis geológico-paleontológica. Suplemento (Adiciones y correcciones)*. 13 pp. Imprenta La Libertad, La Plata.

Ameghino, F. 1902. Première contribution à la connaissance de la faune mammalogique de couches à Colpodon. *Boletín de la Academia Nacional de Ciencias de Córdoba* 17: 71–141.

Ameghino, F. 1904. Recherches de Morphologie philogénétique sur les molaires supérieurs des ongulés. *Anales del Museo Nacional de Buenos Aires* 9 (3): 1–541.

Ankel-Simons, F. 1996. Deciduous dentition of the aye aye, *Daubentonia madagascariensis*. *American Journal of Primatology* 39 (2): 87–97.

Antoine, P.O., Baby, P., Benammi, M., Brusset, S., De Franceschi, D., Espurt, N., Goillot, C., Pujos, F., Salas-Gismondi, R., Tejada, J., and Urbina, M. 2007. The Laventan Fitzcarrald local fauna, Amazonian Peru. *Caudernos del Museo Geominero* 8: 19–24.

Asher, R.J., Gunnell, G.F., Seiffert, E.R., Pattinson, D., Tabuce, R., Hautier, L., and Sallam, H.M. 2017. Dental eruption and growth in Hyracoidea (Mammalia, Afrotheria). *Journal of Vertebrate Paleontology* 37 (3): e1317638.

Bershaw, J., Garzione, C.N., Higgins, P., MacFadden, B.J., Anaya, F., and Alvarenga, H. 2010. Spatial-temporal changes in Andean plateau climate and elevation from stable isotopes of mammal teeth. *Earth and Planetary Science Letters* 289: 530–538.

Billet, G., Patterson, B., and Muizon, C. de 2009. Craniodental anatomy of late Oligocene archaeohyracids (Notoungulata, Mammalia) from Bolivia and Argentina and new phylogenetic hypotheses. *Zoological Journal of the Linnean Society* 155: 458–509.

Blender Online Community 2022. *A 3D Modelling and Rendering Package* [https://www.blender.org]

Bond, M., López, G., and Noriega, J.I. 2001. El primer registro de Uruguaytheriinae (Mammalia, Astrapotheria) de la República Argentina. *Ameghiniana* 38 (4 supplement): 28R.

Bond, M., Reguero, M.A., López, G., Gustavo, J., and Vucetich, M.G. 1998. Los mamíferos de la Formación Fray Bentos (Edad mamífero deseadense, Oligoceno superior?) de las provincias de Corrientes y Entre Ríos, Argentina. *Paleógeno de América del Sur y de la Península Antártica* 5: 41–50.

Bondesio, P., Rabassa, J., Pascual, R., Vucetich, M.G., and Scillato Yané, G. 1980. La Formación Collón Curá de Pilcaniyeu Viejo y sus alrededores (Río Negro, Argentina). Su antigüedad y las condiciones ambientales según su distribución, su litogénesis y sus vertebrados. *2° Congreso Argentino de Paleontología y Bioestratigrafía y 1° Congreso Latinoamericano de Paleontología (Buenos Aires)*, Actas 3: 85–99.

Brandoni, D., Carlini, A.A., Anaya, F., Gans, P., and Croft, D.A. 2018. New remains of *Megathericulus patagonicus* Ameghino, 1904 (Xenarthra, Tardigrada) from the Serravallian (Middle Miocene) of Bolivia; chronological and biogeographical implications. *Journal of Mammalian Evolution* 25: 327–337.

Buk, K. and Knight, M.H. 2010. Seasonal diet preferences of black rhinoceros in three arid South African National Parks. *African Journal of Ecology* 48: 1064–1075.

Butler, P.M. 1937. Studies of the mammalian dentition.—I. The teeth of *Centetes ecaudatus* and its allies. *Proceedings of the Zoological Society of London B* 107: 103–132.

Cabrera, A. 1929. Un astrapoterido de Colombia. *Physis* 9: 436–439.

Cabrera, A. 1940. Sobre dos grandes mamíferos friasenses. *Notas del Museo de La Plata* 5: 241–250.

Cadena, E.A., Anaya, F., and Croft, D.A. 2015. Giant fossil tortoise and freshwater chelid turtles from the Middle Miocene, Quebrada Honda, Bolivia: evidence for lower paleoelevations for the southern Altiplano. *Journal of South American Earth Science* 64: 190–198.

Carmo, G.M., Lima, S.S., Araújo-Júnior, H.I., Pinheiro, R.M., Melo, D.J., and Couto-Ribeiro, G. 2024. Checklist paleofaunístico da Formação Tremembé (Oligoceno da Bacia de Taubaté, Vale do Paraíba, Brasil). *Terrae Didatica* 20: e024013.

Carrillo, J.D., Amazon, E., Jaramillo, C., Sánchez, R., Quiroz, L., Cuartas, C., Rincón, A.F., and Sánchez-Villagra, M.R. 2018. The Neogene record of northern South American native ungulates. *Smithsonian Contributions to Paleobiology* 101: 1–67.

Carrillo, J.D., Jaramillo, C., Abadía, F., Aguilera, O., Alfonso-Rojas, A., Billet, G., Benites-Palomino, A., Cadena, E.-A., Cárdenas, A., Carlini, A.A., Carrillo-Briceño, J., Carvalho, M., Cortés, D., Escobar, J., Herrera, F., Link, A., Luque, J., Martínez, C., Pérez-Lara, D.K., Salas-Gismondi, R., Suarez, C., Stiles, E., Urrea-Barreto, F.J., and Zapata, S. 2023. The Miocene La Venta biome (Colombia): A century of research and future perspectives. *Geodiversitas* 45: 739–767.

Cassini, G.H., Cerdeño, E., Villafañe, A.L., and Muñoz, N.A. 2012. Paleobiology of Santacrucian native ungulates (Meridiungulata; Astrapotheria, Litopterna and Notoungulata). *In:* S.F. Vizcaíno, R.F. Kay, R.F., and M.S. Bargo (eds.), *Early Miocene Paleobiology in Patagonia: High-Latitude Paleocommunities of the Santa Cruz Formation,* 243–286. Cambridge University Press, Cambridge.

Catena, A.M. and Croft, D.A. 2020. What are the best modern analogs for ancient South American mammal communities? Evidence from ecological diversity analysis (EDA). *Palaeontologia Electronica* 23 (1): a03.

Catena, A.M., Hembree, D.I., Saylor, B.Z., Anaya, F., and Croft, D.A. 2016. Paleoenvironmental analysis of the Neotropical fossil mammal site of Cerdas, Bolivia (Middle Miocene) based on ichnofossils and paleopedology. *Palaeogeography, Palaeoclimatology, Palaeoecology* 459: 423–439.

Catena, A.M., Hembree, D.I., Saylor, B.Z., Anaya, F., and Croft, D.A. 2017. Paleosol and ichnofossil evidence for significant Neotropical habitat variation during the late Middle Miocene (Serravallian). *Palaeogeography, Palaeoclimatology, Palaeoecology* 487: 381–398.

The CenCO_2PIP Consortium. 2023. Toward a Cenozoic history of atmospheric CO_2. *Science* 382: eadi5177.

Cerdeño, E. and Schmidt, G.I. 2013. Milk molars or extra premolars in Mesotheriinae (Mesotheriidae, Notoungulata): New insights into an old controversy. *Geobios* 46: 195–202.

Cerdeño, E., Schmidt, G.I., Miño-Boilini, A.R., and Zurita, A. E. 2020. New data on the diversity of Notoungulata (Mammalia) from Fray Bentos formation (late Oligocene) in Corrientes Province, Argentina. *Ameghiniana* 57: 443–461.

Cerling, T.E., Andanje, S.A., Blumenthal, S.A., Brown, F.H., Chritz, K.L., Harris, J.M., Hart, J.A., Kirera, F.M., Kaleme, P., Leakey, L.N., Leakey, M.G., Levin, N.E., Manthi, F.K., Passey, B.H., and Uno, K.T. 2015. Dietary changes of large herbivores in the Turkana Basin, Kenya from 4 to 1 Ma. *Proceedings of the National Academy of Sciences* 112: 11467–11472.

Cerling, T.E., Chritz, K.L., Jablonski, N.G., Leakey, M.G., and Manthi, F.K. 2013. Diet of *Theropithecus* from 4 to 1 Ma in Kenya. *Proceedings of the National Academy of Sciences* 110: 10507–10512.

Cifelli, R.L. 1993. The phylogeny of the native South American ungulates. *In:* F.S. Szalay, M.J. Novacek, M.J., and M.C. McKenna (eds.), *Mammal Phylogeny: Placentals,* 195–216. Springer-Verlag, New York.

Croft, D.A. 2007. The Middle Miocene (Laventan) Quebrada Honda Fauna, southern Bolivia, and a description of its notoungulates. *Palaeontology* 50: 277–303.

Croft, D.A. 2016. *Horned Armadillos and Rafting Monkeys: The Fascinating Fossil Mammals of South America*. 320 pp. Indiana University Press, Bloomington, Indiana.

Croft, D.A. and Anaya, F. 2006. A new Middle Miocene hegetotheriid (Notoungulata: Typotheria) and a phylogeny of the Hegetotheriidae. *Journal of Vertebrate Paleontology* 26: 387–399.

Croft, D.A. and Anaya, F. 2020. A new typothere notoungulate (Mammalia: Interatheriidae), from the Miocene Nazareno Formation of southern Bolivia. *Ameghiniana* 57: 189–208.

Croft, D.A., Anaya F., Auerbach D., Garzione C., and MacFadden B.J. 2009. New data on Miocene Neotropical provinciality from Cerdas, Bolivia. *Journal of Mammalian Evolution* 16: 175–198.

Croft, D.A., Carlini, A.A., Ciancio, M.R., Brandoni, D., Drew, N.E., Engelman, R.K., and Anaya, F. 2016. New mammal faunal data from Cerdas, Bolivia, a middle-latitude neotropical site that chronicles the end of the Middle Miocene climatic optimum in South America. *Journal of Vertebrate Paleontology* 36 (5): e1163574.

Croft, D.A., Chick, J., and Anaya, F. 2011. New Middle Miocene caviomorph rodents from Quebrada Honda, Bolivia. *Journal of Mammalian Evolution* 18: 245–268.

Croft, D.A., Flynn, J.J., and Wyss, A.R. 2004 Notoungulata and Litopterna of the Early Miocene Chucal Fauna, northern Chile. *Fieldiana Geology* 50: 1–52.

Croft, D.A., Flynn, J.J., and Wyss, A.R. 2007. A new basal glyptodontid and other Xenarthra of the Early Miocene Chucal Fauna, northern Chile. *Journal of Vertebrate Paleontology* 27: 781–797.

Croft, D.A., Gelfo, J.N., and López, G.M. 2020a. Splendid innovation: the extinct South American native ungulates. *Annual Review of Earth and Planetary Sciences* 48: 259–290.

Croft, D.A., Martinez, J., and Tapia, P.M. 2020b. The first record of a Miocene terrestrial mammal (Astrapotheria: Uruguaytheriinae) from northern coastal Peru. *Ameghiniana* 57: 146–158.

Damuth, J. and Janis, C.M. 2011. On the relationship between hypsodonty and feeding ecology in ungulate mammals, and its utility in palaeoecology. *Biological Reviews* 86: 733–758.

Damuth, J. and MacFadden, B.J. 1990. Body Size in Mammalian Paleobiology: Estimation and Biological Implications. *Cambridge University Press, Cambridge*.

de Deus Vidal, J., Jr., le Roux, P.C., Johnson, S.D., te Beest, M., and Clark, V.R. 2021. Beyond the tree-line: the C3–C4 "grass-line" can track global change in the world's grassy mountain systems. *Frontiers in Ecology and Evolution* 9: 760118.

Edwards, E.J., Osborne, C.P., Strömberg, C.A.E., and Smith, S.A. 2010. The origins of C4 grasslands: integrating evolutionary and ecosystem science. *Science* 328: 587–591.

Engelman, R.K., Anaya, F., and Croft, D.A. 2017. New palaeothentid marsupials (Paucituberculata) from the Middle Miocene of Quebrada Honda, Bolivia, and their implications for the palaeoecology, decline and extinction of the Palaeothentoidea. *Journal of Systematic Palaeontology* 15: 787–820.

Engelman, R.K., Anaya, F., and Croft, D.A. 2020. *Australogale leptognathus,* gen. et sp. nov., a second species of small sparassodont (Mammalia, Metatheria) from the Middle Miocene locality of Quebrada Honda, Bolivia. *Journal of Mammalian Evolution* 27: 37–54.

Engelman, R.K. and Croft, D.A. 2014. A new species of small-bodied sparassodont (Mammalia: Metatheria) from the Middle Miocene locality of Quebrada Honda, Bolivia. *Journal of Vertebrate Paleontology* 34: 672–688.

Fernández-Monescillo, M., Antoine, P.-O., Mamani Quispe, B., Münch, P., Andradre Flores, R., Marivaux, L., and Pujos, F. 2019. Multiple skeletal and dental pathologies in a Late Miocene mesotheriid (Mammalia, Notoungulata) from the Altiplano of Bolivia: Palaeoecological inferences. *Palaeogeography, Palaeoclimatology, Palaeoecology* 534: 109297.

Flynn, J.J., Croft, D.A., Charrier, R., Hérail, G., and Wyss, A. R. 2002. The first Cenozoic mammal fauna from the Chilean Altiplano. *Journal of Vertebrate Paleontology* 22: 200–206.

Folino, M., Dozo, M.T., Martínez, G., and Vera, B. 2024. New insights into the upper and lower deciduous dentition of *Pyrotherium* from the late Oligocene of South America. *Journal of Mammalian Evolution* 31 (4): 40.

Forasiepi, A.M., Martinelli, A.G., de la Fuente, M.S., Dieguez, S., and Bond, M. 2011. Paleontology and stratigraphy of the Aisol Formation (Neogene), San Rafael, Mendoza. *In*: J.A. Salfity and R.A. Marquillas (eds.), *Cenozoic Geology of the Central Andes of Argentina*, 135–154. SCS Publisher, Salta, Argentina.

Forasiepi, A.M., Sánchez-Villagra, M.R., Goin, F.J., Takai, M., Shigehara, N., and Kay, R.F. 2006. A new species of Hathliacynidae (Metatheria, Sparassodonta) from the Middle Miocene of Quebrada Honda, Bolivia. *Journal of Vertebrate Paleontology* 26: 670–684.

Frailey, C.D. 1987. The Miocene vertebrates of Quebrada Honda, Bolivia. Part I. Astrapotheria. *Occasional Papers of the Museum of Natural History, The University of Kansas* 122: 1–15.

Frailey, C.D. 1988. The Miocene vertebrates of Quebrada Honda, Bolivia. Part II. Edentata. *Occasional Papers of the Museum of Natural History, The University of Kansas* 123: 1–13.

Francis, J.C. 1965. Los géneros de la subfamilia Mesotheriinae (Typotheria, Notoungulata) de la República Argentina. *Boletin del Laboratorio de Paleontología de Vertebrados* 1 (1): 7–31.

Garzione, C.N., Hoke, G.D., Libarkin, J.C., Withers, S., MacFadden, B., Eiler, J., Ghosh, P., and Mulch, A. 2008. Rise of the Andes. *Science* 320: 1304–1307.

Garzione, C.N., Auerbach, D.J., Smith, J.J.-S., Rosario, J.J., Passey, B.H., Jordan, T.E., and Eiler, J.M. 2014. Clumped isotope evidence for diachronous surface cooling of the Altiplano and pulsed surface uplift of the Central Andes. *Earth and Planetary Science Letters* 393: 173–181.

Garzione, C.N., McQuarrie, N., Perez, N.D., Ehlers, T.A., Beck, S.L., Kar, N., Eichelberger, N., Chapman, A.D., Ward, K.M., Ducea, M.N., Lease, R.O., Poulsen, C.J., Wagner, L.S., Saylor, J.E., Zandt, G., and Horton, B.K. 2017. Tectonic evolution of the Central Andean Plateau and implications for the growth of plateaus. *Annual Review of Earth and Planetary Sciences* 45: 529–559.

Gmelin, J.F. 1788. *Systema Naturae per Regna Tria Naturae, Secundum Classes, Ordines, Genera, Species, cum characteribus, diHerentiis, synonymis, locis. Tomus I*. 500 pp. Georg Emanuel Beer, Leipzig.

Gibert, L., Deino, A., Valero, L., Anaya, F., Lería, M., Saylor, B.Z., and Croft, D.A. 2020. Chronology of Miocene terrestrial deposits and fossil vertebrates from Quebrada Honda (Bolivia). *Palaeogeography, Palaeoclimatology, Palaeoecology* 560: 110013.

Goddard, J. 1970. Food preferences of black rhinoceros in the Tsavo National Park. *African Journal of Ecology* 8: 145–161.

Goillot, C., Antoine, P., Tejada, J., Pujos, F., and Salas Gismondi, R. 2011. Middle Miocene Uruguaytheriinae (Mammalia, Astrapotheria) from Peruvian Amazonia and a review of the astrapotheriid fossil record in northern South America. *Geodiversitas* 33: 331–345.

Goin, F. J., Sánchez-Villagra, M.R., Kay, R. F., Anaya-Daza, F., and Takai, M. 2003. New palaeothentid marsupial from the Middle Miocene of Bolivia. *Palaeontology* 46: 307–315.

Gregory-Wodzicki, K.M. 2000. Uplift history of the Central and Northern Andes: a review. *Geological Society of America Bulletin* 112: 1091–1105.

Gregory-Wodzicki, K.M. 2002. A Late Miocene subtropical-dry flora from the northern Altiplano, Bolivia. *Palaeogeography, Palaeoclimatology, Palaeoecology* 180: 331–348.

Hernesniemi, E., Blomstedt, K., and Fortelius, M. 2011. Multi-view stereo three-dimensional reconstruction of lower molars of recent and Pleistocene rhinoceroses for mesowear analysis. *Palaeontologia Electronica* 14 (2): 2T.

Hoerner, M.E. 2017. *The Ecological and Evolutionary Dynamics of Species Introductions and Environmental Change: From East African Cichlids to the Great American Biotic Interchange*. 1105 pp. The University of Chicago, Chicago.

Hoffstetter, R. 1977. Un gisement de Mammifères miocènes à Quebrada Honda (Sud Bolivien). *Comptes Rendus de la Académie des Sciences, Paris, Sèrie D* 284: 1517–1529.

Houssaye, A., Fernandez, V., and Billet, G. 2016. Hyperspecialization in some South American endemic ungulates revealed by long bone microstructure. *Journal of Mammalian Evolution* 23: 221–235.

Hynek, S.A., Passey, B.H., Prado, J.L., Brown, F.H., Cerling, T.E., and Quade, J. 2012. Small mammal carbon isotope ecology across the Miocene–Pliocene boundary, northwestern Argentina. *Earth and Planetary Science Letters* 321–322: 177–188.

Janis, C.M. 1988. An estimation of tooth volume and hypsodonty indices in ungulate mammals, and the correlation of these factors with dietary preference. *Mémoires du Museum National d´Historie Naturelle* 53: 367–387.

Janis, C.M. and Fortelius, M. 1988. On the means whereby mammals achieve increased functional durability of their dentitions, with special reference to limiting factors. *Biological Reviews* 63: 197–230.

Johnson, S.C. 1984. *Astrapotheres from the Miocene of Colombia, South America*. 182 pp. Ph.D., University of California, Berkley.

Johnson, S.C. and Madden, R.H. 1997. Uruguaytheriine astrapotheres of tropical South America. *In:* R.F. Kay, R.H. Madden, R.L. Cifelli, and J.J. Flynn (eds.), *Vertebrate Paleontology in the Neotropics: The Miocene Fauna of La Venta*, 355–381. Smithsonian Institution Press, Washington, D.C.

Kaiser, T.M., Müller, D.W.H., Fortelius, M., Schulz, E., Codron, D., and Clauss, M. 2013. Hypsodonty and tooth facet development in relation to diet and habitat in herbivorous ungulates: Implications for understanding tooth wear. *Mammal Review* 43: 34–46.

Kay, R.F. and Madden, R.H. 1997. Mammals and rainfall: paleoecology of the Middle Miocene at La Venta (Colombia, South America). *Journal of Human Evolution* 32: 161–199.

Kay, R.F., Madden, R.H., Cifelli, R.L., and Flynn, J.J. 1997. *Vertebrate Paleontology in the Neotropics: the Miocene Fauna of La Venta, Colombia*. 592 pp. Smithsonian Institution Press, Washington, D.C.

Kay, R.F., MacFadden, B.J., Madden, R.H., Sandeman, H., and Anaya, F. 1998. Revised age of the Salla beds, Bolivia, and its bearing on the age of the Deseadan South American Land Mammal "Age". *Journal of Vertebrate Paleontology* 18: 189–199.

Kotze, D.C. and Zacharias, P.J.K. 1993. Utilization of woody browse and habitat by the black rhino (*Diceros bicornis*) in western Itala Game Reserve. *African Journal of Range and Forage Science* 10: 36–40.

Kraglievich, L. 1928. *Sobre el supuesto Astrapotherium christi Stehlin, decubierto en Venezuela, (*Xenastrapotherium *n. gen.) y sus relaciones con* Astrapotherium magnum *y* Uruguaytherium Beaulieui. 16 pp. La Editorial Franco, Buenos Aires.

Kraglievich, L. 1930. La Formatión Friaseana del Río Frías, Río Fénix, Laguna Blanca, etc. y su fauna de mamíferos. *Physis* 10: 127–61.

Kramarz, A.G. 2009. Adiciones al conocimiento de *Astrapothericulus* (Mammalia, Astrapotheria): anatomía cráneo-dentaria, diversidad y distribución. *Revista Brasileira de Paleontologia* 12 (1): 55–66.

Kramarz, A.G. and Bond, M. 2008. Revision of *Parastrapotherium* (Mammalia, Astrapotheria) and other Deseadan astrapotheres of Patagonia. *Ameghiniana* 45: 547–551.

Kramarz, A.G. and Bond, M. 2009. A new Oligocene astrapothere (Mammalia, Meridiungulata) from Patagonia and a new appraisal of astrapothere phylogeny. *Journal of Systematic Palaeontology* 7: 117–128.

Kramarz, A. and Bond, M. 2010. Colhuehuapian Astrapotheriidae (Mammalia) from Gran Barranca south of Lake Colhue-Huapi. *In:* R.H. Madden, A.A. Carlini, M.G. Vucetich, and R.F. Kay (eds.), *The Paleontology of Gran Barranca Evolution and Environmental Change through the Middle Cenozoic of Patagonia,* 182–192. Cambridge University Press, Cambridge.

Kramarz, A.G. and Bond, M. 2011. A new Early Miocene astrapotheriid (Mammalia, Astrapotheria) from Northern Patagonia, Argentina. *Neues Jahrbuch für Geologie und Paläontologie, Abhandlungen* 260: 277–287.

Kramarz, A.G., Bond, M., and Forasiepi, A.M. 2011. New remains of *Astraponotus* (Mammalia, Astrapotheria) and considerations on Astrapothere cranial evolution. *Paläontologische Zeitschrift* 85: 185–200.

Kramarz, A., Garrido, A., and Bond, M. 2019. *Astrapotherium* from the Middle Miocene Collón Cura formation and the decline of astrapotheres in southern South America. *Ameghiniana* 56: 290–306.

Laurie, W.A., Land, E.M., and Groves, C.P. 1983. *Rhinoceros unicornis*. *Mammalian Species* 211 (15): 1–6.

Linnaeus, C. 1758. *Systema naturæ per regna tria naturæ, secundum classes, ordines, genera, species, cum characteribus, differentiis, synonymis, locis. Tomus I. Editio decima, reformata*. 824 pp. Laurentius Salvius, Stockholm.

Loutit, B.D., Louw, G.N., and Seely, M.K. 1987. First approximation of food preferences and the chemical composition of the diet of the desert-dwelling black rhinoceros, *Diceros bicornis* L. *Madoqua* 15 (1): 35–54.

Lydekker, R. 1894. Contributions to a knowledge of the fossil vertebrates of Argentina. 3. A study of extinct Argentine ungulates. *Anales del Museo de La Plata. Paleontología Argentina* 2 (3): 1–91.

Mercerat, A. 1891. Notas sobre la paleontología de la República Argentina. II. Sinopsis de la familia de los Protoxodontidae conservados en el Museo de La Plata (Eoceno de Patagonia). *Revista del Museo de La Plata (Nueva Serie)* 1: 382–444.

MacFadden, B.J. and Higgins, P. 2004. Ancient ecology of 15-million-year-old browsing mammals within C3 plant communities from Panama. *Oecologia* 140 (1): 169–182.

MacFadden, B.J., Anaya, F., Perez, H., Naeser, C.W., Zeitler, P.K., and Campbell Jr., K.E. 1990. Late Cenozoic paleomagnetism and chronology of Andean Basins of Bolivia: evidence for possible oroclinal bending. *Journal of Geology* 98: 541–555.

MacFadden, B.J., Anaya, F., and Swisher, C.C., III. 1995. Neogene paleomagnetism and oroclinal bending of the central Andes of Bolivia. *Journal of Geophysical Research* 100 (B5): 8153–8167.

MacFadden, B.J., Campbell Jr., K.E., Cifelli, R.L., Siles, O., Johnson, N.M., Naeser, C.W., and Zeitler, P.K. 1985. Magnetic polarity stratigraphy and mammalian fauna of the Deseadan (late Oligocene–Early Miocene) Salla beds of northern Bolivia. *The Journal of Geology* 93: 223–250.

MacFadden, B.J., Cerling, T.E., and Prado, J. 1996. Cenozoic terrestrial ecosystem evolution in Argentina: Evidence from carbon isotopes of fossil mammal teeth. *Palaios* 11: 319–327.

MacFadden, B.J., Wang, Y., Cerling, T.E., and Anaya, F. 1994. South American fossil mammals and carbon isotopes: a 25 million-year sequence from the Bolivian Andes. *Palaeogeography, Palaeoclimatology, Palaeoecology* 107: 257–268.

MacFadden, B.J. and Wolff, R.G. 1981. Geological investigations of Late Cenozoic vertebrate-bearing deposits in southern Bolivia. *Anais do II Congresso Latino-Americano de Paleontología* 2: 765–778.

Madden, R.H., Guerrero, J., Kay, R.F., Flynn, J.J., Swisher, C.C., and Walton, A.H. 1997. The Laventan stage and age *In*: R.F. Kay, R.H. Madden, R.L. Cifelli, and J.J. Flynn (eds.), *Vertebrate Paleontology in the Neotropics. The Miocene Fauna of La Venta, Colombia*, 499–519. Smithsonian Institution Press, Washington, D.C.

Marshall, L.G., Salinas, P., and Suárez, M. 1990. *Astrapotherium* sp. (Mammalia, Astrapotheriidae) from Miocene strata along the Quepuca River, central Chile. *Revista Geológica de Chile* 17: 215–223.

Marshall, L.G. and Sempere, T. 1991. The Eocene to Pleistocene vertebrates of Bolivia and their stratigraphic context: a review. *In*: R. Suárez-Soruco (ed.), *Fósiles y Facies de Bolivia. Vol. I: Vertebrados*, 631–652. Yacimientos Petrolíferos Fiscales Bolivianos, Santa Cruz.

McGrath, A.J., Anaya, F., and Croft, D.A. 2018. Two new macraucheniids (Mammalia: Litopterna) from the late Middle Miocene (Laventan South American Land Mammal Age) of Quebrada Honda, Bolivia. *Journal of Vertebrate Paleontology* 38: e1461632.

McGrath, A.J., Anaya, F., and Croft, D.A. 2020. New proterotheriids (Litopterna, Mammalia) from the Middle Miocene of Quebrada Honda, Bolivia, and trends in diversity and body size of proterotheriid and macraucheniid litopterns. *Ameghiniana* 52: 159–188.

McGrath, A.J., Flynn, J.J., Croft, D.A., Chick, J., Dodson, H.E., and Wyss, A.R. 2023. Caviomorphs (Rodentia, Hystricognathi) from Pampa Castillo, Chile: new octodontoid records and biochronological implications. *Papers in Palaeontology* 9 (1): e1477.

Mendoza, M., Janis, C.M., and Palmqvist, P. 2002. Characterizing complex craniodental patterns related to feeding behaviour in ungulates: a multivariate approach. *Journal of Zoology* 258: 223–246.

Mones, A. and Ubilla, M. 1978. La Edad deseadense (Oligoceno Inferior) de la Formacion Fray Bentos y su contenido paleontologico, con especial referencia a la presencia de *Proborhyaena cf. gigantea* Ameghino (Marsupialia: Borhyaenidae) en el Uruguay. Nota preliminar. *Comunicaciones Paleontológicas del Museo de Historia Natural de Montevideo* 1 (7): 151–158.

Negri, F.R., Bocquentin-Villanueva, J., Ferigolo, J., and Antoine, P.O. 2010. A review of Tertiary mammal faunas and birds from western Amazonia *In:* C. Hoorn and F.P. Wesselingh (eds.), *Amazonia: Landscape and Species Evolution*, 243–258. Blackwell Publishing Ltd., West Sussex.

Nelson, A., Engelman, R., and Croft, D. 2023. How to weigh a fossil mammal? South American notoungulates as a case study for estimating body mass in extinct clades. *Journal of Mammalian Evolution* 30: 773–809.

Nowak, R.M. 1991. *Walker's Mammals of the World (Fifth Edition)*. The Johns Hopkins University Press, Baltimore.

Ogg, J.G. 2012. Geomagnetic polarity time scale. *In:* F.M. Gradstein, F.M. and J.G. Ogg (eds.), *The Geological Time Scale*, 85–113. Elsevier, Amsterdam.

Oiso, Y. 1991. New land mammal locality of Middle Miocene (Colloncuran) age from Nazareno, southern Bolivia. *In*: R. Suárez-Soruco (ed.), *Fósiles y Facies de Bolivia. Vol. I: Vertebrados*, 653–672. Yacimientos Petrolíferos Fiscales Bolivianos, Santa Cruz.

Owen, F.R.S. 1853. Description of some species of the extinct genus *Nesodon* with remarks on the primary group (Toxodontia) of the hoofed quadrupeds to which that genus is referable. *Philosophical Transactions of the Royal Society of London* 143: 291–310.

Pallas, P.S. 1766. *Miscellanea Zoologica Quibus novæ imprimis atque obscuræ Animalium Species describuntur et observationibus iconibusque illustrantur*. 224 pp. Petrus van Cleef, The Hague.

Pardo-Jaramillo, M. 2018. Reporte del hallazgo de restos de *Hilarcotherium* sp. (Mammalia, Astrapotheria) y de material asociado en una nueva localidad fosilífera del valle inferior del Magdalena, ciénaga de Zapatosa, Cesar, Colombia. *Revista de la Academia Colombiana de Ciencias Exactas, Físicas y Naturales* 42 (164): 280–286.

Patterson, B. and Pascual, R. 1968. The fossil mammal fauna of South America. *Quarterly Review of Biology* 43: 409–451.

Patterson, B. and Wood, A.E. 1982. Rodents from the Deseadan Oligocene of Bolivia and the relationships of the Caviomorpha. *Bulletin of the Museum of Comparative Zoology* 149: 371–543.

Paula Couto, C. de 1976. Fossil mammals from the Cenozoic of Acre, Brazil. I. Astrapotheria. *Anais do XXVIII Congresso Brasileiro de Geologia*: 237–248. Sociedade Brasileira de Geologia, Porto Alegre.

Paula Couto, C. de 1979. Ungulados fósseis do Riochiquense de Itaboraí, RJ, Brasil. IV – Retificação sobre os Notoungulata. *Anais da Academia Brasileira de Ciencias* 51 (2): 345–348.

Paula Couto, C. de 1982. Fossil mammals from the Cenozoic of Acre, Brazil. V. Notoungulata Nesodontinae (II), Toxodontinae and Haplodontheriinae, and Litopterna, Pyrotheria and Astrapotheria (II). *Iheringia, Série Geología* 7: 5–43.

Perea, D., Toriño, P., and Ciancio, M.R. 2014. La presencia del Xenarto *Palaeopeltis inornatus* Ameghino, 1894, en la Formación Fray bentos (oligoceno Tardío), Uruguay. *Ameghiniana* 51: 254–258.

Perkins, M.E., Fleagle, J.G., Heizler, M.T., Nash, B., Bown, T.M., Tauber, A.A., and Dozo, M.T. 2012. Tephnochronology of the Miocene Santa Cruz and Pinturas formations, Argentina. *In*: S.F. Vizcaíno, R.F. Kay, and M.S. Bargo (eds.), *Early Miocene Paleobiology in Patagonia: High-Latitude Paleocommunities of the Santa Cruz Formation*, 23–40. Cambridge University Press, Cambridge.

Polycam Inc. 2024. *Polycam* [https://poly.cam/]

Popowics, T.E. and Fortelius, M.F. 1997. On the cutting edge: Tooth blade sharpness in herbivorous and faunivorous mammals. *Annales Zoologici Fennici* 34: 73–88.

Pujos, F., De Iuliis, G., and Quispe, B.M. 2011. *Hiskatherium saintandrei*, gen. et sp. nov.: an unusual sloth from the Laventan of Quebrada Honda (Bolivia) and an overview of Middle Miocene, small megatherioids. *Journal of Vertebrate Paleontology* 31: 1131–1149.

Pujos, F., De Iuliis, G., Quispe, B.M., and Flores, R.A. 2014. *Lakukullus anatisrostratus*, gen. et sp. nov., a new massive nothrotheriid sloth

(Xenarthra, Pilosa) from the Middle Miocene of Bolivia. *Journal of Vertebrate Paleontology* 35: 1243–1248.

Ranzi, A. 1981. *Mamíferos fósseis do Cenozóico do Alto Juruá – Acre*. 327 pp. Unpublished Thesis, Universida de Federal do Rio Grande Do Sul, Porto Alegre.

Ranzi, A. 2008. *Paleontologia da Amazônia: Mamíferos e Fosseis do Juruá*. 130 pp. M.M. PAIM, Rio Branco.

Reguero, M.A., Ubilla, M., and Perea, D. 2003. A new species of *Eopachyrucos* (Mammalia, Notoungulata, Interatheriidae) from the Late Oligocene of Uruguay. *Journal of Vertebrate Paleontology* 23: 445–457.

Rensberger, J.M. and Pfretzschner, H.U. 1992. Enamel structure in astrapotheres and its functional implications. *Scanning Microscopy* 6: 495–510.

Rensberger, J.M. 2004. Evidence from the enamel microstructure for reversals in dietary behavior in the transition from primitive Ceratomorpha to Rhinocerotoidea. *Bulletin of Carnegie Museum of Natural History* 36: 199–210.

Riggs, E.S. 1935. A skeleton of *Astrapotherium*. *Geological Series, Field Museum of Natural History* 6 (13): 167–176.

Ritchie, A.T.A. 1963. The black rhinoceros (*Diceros bicornis* L.). *African Journal of Ecology* 1: 54–62.

Roig, M, Miño-Boilini, A.R., and Schmidt, G. 2024. Vertebrados continentals del Oligoceno tardío de las provincias de Corrientes y Entre Ríos, Argentina. *Pulicación Electrónica de la Asociación Paleontológica Argentina* 24(R4): R44.

Rookmaaker, K. and Antoine, P.-O. 2012. New maps representing the historical and recent distribution of the African species of rhinoceros: *Diceros bicornis*, *Ceratotherium simum* and *Ceratotherium cottoni*. *Pachyderm* 52: 91–96.

Saarinen, J. and Lister, A.M. 2023. Fluctuating climate and dietary innovation drove ratcheted evolution of proboscidean dental traits. *Nature Ecology and Evolution* 7: 1490–1502.

Sánchez-Villagra, M.R., Kay, R.F., and Anaya-Daza, F. 2000. Cranial anatomy and palaeobiology of the Miocene marsupial *Hondalagus altiplanensis* and a phylogeny of argyrolagids. *Palaeontology* 43: 287–301.

Saylor, B.Z., Catena, A.M., Hembree, D.I., Anaya, F., and Croft, D.A. 2022. Lithostratigraphy, chronostratigraphy, and sedimentary environments of the Middle Miocene Quebrada Honda Basin in southern Bolivia and implications for Andean climate and uplift. *Palaeogeography, Palaeoclimatology, Palaeoecology* 601: 111135.

Schneider, C.A., Rasband, W.S., and Eliceiri, K.W. 2012. NIH Image to ImageJ: 25 years of image analysis. *Nature Methods* 9: 671–675.

Schreber, J.C.D. von. 1777. Plate 165. *In*: J.C.D. von Schreber 1774–1855. *Die Säugthiere in Abbildungen nach der Natur, mit Beschreibungen*. Walther, Erlangen.

Scott, W.B. 1928. Mammalia of the Santa Cruz Beds. Volume VI, Paleontology. Part IV, Astrapotheria. *In*: W.B. Scott (ed.), *Reports of the Princeton University Expeditions to Patagonia, 1896–1899*, 301–341. Princeton University, E. Schweizerbart'sche Verlagshandlung (E. Nägele), Stuttgart.

Scott, W.B. 1937. The Astrapotheria. *Proceedings of the American Philosophical Society* 77: 309–393.

Shockey, B.J. 1997. *Toxodontia of Salla, Bolivia (Late Oligocene): Taxonomy, Systematics, and Functional Morphology*. 275 pp. Ph.D. Dissertation, University of Florida, Gainesville.

Shockey, B.J. and Anaya, F. 2008. Postcranial osteology of mammals from Salla, Bolivia (late Oligocene): form, function, and phylogenetic implications. *In*: E.J. Sargis and M. Dagosto (eds.), *Mammalian Evolutionary Morphology: A Tribute to Frederick S. Szalay*, 135–157. Springer, New York.

Simpson, G.G. 1980. *Splendid Isolation: the Curious History of South American Mammals*. 266 pp. Yale University Press, New Haven, Connecticut.

Soria, M.F. 1983. Vertebrados fósiles y edad de la Formación Aisol, provincia de Mendoza. *Revista de la Asociación Geológica Argentina* 38: 299–306.

Soria, M.F. 1984. Eoastrapostylopidae: diagnosis e implicaciones en la sistemática y evolución de los Astrapotheria preoligocénicos. *In*: *Actas 2 Congreso Argentino de Paleontología y Bioestratigrafía*, 175–182. Asociación Paleontológica Argentina, Buenos Aires.

Stehlin, H.G. 1928. Ein Astrapotheriumfund aus Venezuela. *Eclogae Geologicae Helvetiae* 21: 227–232.

Stirton, R.A. 1947. The first Oligocene mammalian fauna from northern South America. *AAPG Bulletin* 30 (1): 327–341.

Strömberg, C.A.E., Saylor, B.Z., Engelman, R.K., Catena, A.M., Hembree, D.I., Anaya, F., and Croft, D.A. 2024. The flora, fauna, and paleoenvironment of the late Middle Miocene Quebrada Honda Basin, Bolivia (Eastern Cordillera, Central Andes). *Palaeogeography, Palaeoclimatology, Palaeoecology* 656: 112518.

Teeri, J.A. and Stowe, L.G. 1976. Climatic patterns and the distribution of C4 grasses in North America. *Oecologia* 23 (1): 1–12.

Tejada-Lara, J.V., MacFadden, B.J., Bermudez, L., Rojas, G., Salas-Gismondi, R., and Flynn, J.J. 2018. Body mass predicts isotope enrichment in herbivorous mammals. *Proceedings of the Royal Society B: Biological Sciences* 285 (1881): 20181020.

Tejada-Lara, J.V., Salas-Gismondi, R., Pujos, F., Baby, P. Benammi, M., Brusset, S., De Franceschi, D., Espurt, N., Urbina, M., and Antoine, P. 2015. Life in proto-Amazonia: Middle Miocene mammals from the Fitzcarrald Arch (Peruvian Amazonia). *Palaeontology* 58: 341–378.

The CenCO_2PIP Consortium. 2023. Toward a Cenozoic history of atmospheric CO_2. *Science* 382 (6675): eadi5177.

Townsend, K.E. and Croft, D.A. 2010. Middle Miocene mesotheriine diversity at Cerdas, Bolivia, and a reconsideration of *Plesiotypotherium minus*. *Palaeontologia Electronica* 13 (1): 1A: 36 pp.

Vallejo-Pareja, M.C., Carrillo, J.D., Moreno-Bernal, J.W., Pardo-Jaramillo, M., Rodriguez-Gonzalez, D.F., and Muñoz-Duran, J. 2015. *Hilarcotherium castanedaii*, gen. et sp. nov., a new Miocene astrapothere (Mammalia, Astrapotheriidae) from the upper Magdalena Valley, Colombia. *Journal of Vertebrate Paleontology* 35 (2): e903960.

Villarroel, C. 1978. Edades y correlaciones de algunas unidades litoestratigráficas del Altiplano boliviano y estudio de algunos representantes mesotériinos. *Revista de la Academía Nacional de Ciencias de Bolivia* 1 (1): 159–170.

Villarroel, C.A. and Marshall, L.G. 1988. A new Argyrolagoid (Mammalia: Marsupialia) from the Middle Miocene of Bolivia. *Journal of Paleontology* 62: 463–467.

Wall, W.P. 1980. Cranial evidence for a proboscis in *Cadurcodon* and a review of snout structure in the family Amynodontidae (Perissodactyla, Rhinocerotoidea). *Journal of Paleontology* 54: 968–977.

Ward, C.T., Crowley, B.E., and Secord, R. 2024. Home on the range: A multi-isotope investigation of ungulate resource partitioning at Ashfall Fossil Beds, Nebraska, USA. *Palaeogeography, Palaeoclimatology, Palaeoecology* 650: 112375.

Weston, E.M., Madden, R.H., and Sánchez-Villagra, M.R. 2004. Early Miocene astrapotheres (Mammalia) from northern South America. *Special Papers in Palaeontology* 71: 81–97.

Wilson, O.E. and Saarinen, J. 2024a. Application of Kurténian theories to non-analogue communities: dental traits in South America. *Annales Zoologici Fennici* 61: 433–454.

Wilson, O.E. and Saarinen, J. 2024b. Mesowear analysis of *Taubatherium paulacoutoi* (Late Oligocene Tremembé Formation, São Paulo State, Brazil). *Revista Brasileira de Paleontologia* 27: e20240454.

Wilson, O.E., Sánchez, R., Chávez-Aponte, E., Carrillo-Briceño, J.D., Saarinen, J. 2024 Application of herbivore ecometrics to reconstruct Neogene terrestrial palaeoenvironments in Falcón, Venezuela. *Palaeogeography, Palaeoclimatology, Palaeoecology* 651: 112397.

Xafis, A., Saarinen, J., Bastl, K., Nagel, D., and Grímsson, F. 2020. Palaeodietary traits of large mammals from the Middle Miocene of Gračanica (Bugojno Bsain, Bosnia-Herzegovina). *Palaeobiodiversity and Palaeoenvironments* 100: 457–477.

Zurita, A.E., González-Ruiz, L.R., Miño-Boilini, A.R., Herbst, R., Scillato-Yané, G.J., and Cuaranta, P. 2016. Paleogene Glyptodontidae Propalaeholophorinae (Mammalia, Xenarthra) in extra-Patagonian areas. *Andean Geology* 43 (1): 127–136.